Austin Research Associates
1901 Rutland Drive - Austin, Texas 78758 - Phone (512) 837-6623

I-ARA-83-U-62 (ARA-502)

FINAL TECHNICAL REPORT FOR THEORETICAL STUDIES ON FREE ELECTRON LASERS

for Period 1 October 1982 - 30 September 1983

M. N. Rosenbluth, H. Vernon Wong and B. N. Moore

November 1983

Sponsored by
Advanced Research Projects Agency (DoD)
ARPA Order No. 3923-11
Monitored by NP
Under Contract No. F49620-81-C-0077

The views and conclusions contained in this document are those of the authors and should not be interpreted as necessarily representing the official policies, either expressed or implied, of the Defense Advanced Research Projects Agency or the U. S. Government.

Approved for public release; distribution unlimited.

Austin Research Associates
1901 Rutland Drive - Austin, Texas 78758 - Phone (512) 837-6623

I-ARA-83-U-62 (ARA-502)

FINAL TECHNICAL REPORT FOR THEORETICAL STUDIES ON FREE ELECTRON LASERS

for Period 1 October 1982 - 30 September 1983

M. N. Rosenbluth, H. Vernon Wong and B. N. Moore

November 1983

Sponsored by
Advanced Research Projects Agency (DoD)
ARPA Order No. 3923-11
Monitored by NP
Under Contract No. F49620-81-C-0077

UNCLASSIFIED

SECURITY CLASSIFICATION OF THIS PAGE (When Data Entered)

REPORT DOCUMENTATION PAGE	READ INSTRUCTIONS BEFORE COMPLETING FORM
1. REPORT NUMBER: AFOSR-TR- 83-1204	2. GOVT ACCESSION NO.: AD-A136 333
3. RECIPIENT'S CATALOG NUMBER	
4. TITLE (and Subtitle): Theoretical Studies on Free Electron Lasers	5. TYPE OF REPORT & PERIOD COVERED: Final Technical Report, 1 Oct. 1982 - 30 Sept. 1983
6. PERFORMING ORG. REPORT NUMBER: I-ARA-83-U-62 (ARA-502)	
7. AUTHOR(s): M. N. Rosenbluth, H. Vernon Wong and B. N. Moore	8. CONTRACT OR GRANT NUMBER(s): F49620-81-C-0077
9. PERFORMING ORGANIZATION NAME AND ADDRESS: Austin Research Associates, 1901 Rutland Drive, Austin, Texas 78758	10. PROGRAM ELEMENT, PROJECT, TASK AREA & WORK UNIT NUMBERS: 2301/A1, 61102F
11. CONTROLLING OFFICE NAME AND ADDRESS: AFOSR/NP, BOLLING AFB, DC 20332	12. REPORT DATE: November 1983
	13. NUMBER OF PAGES: 128
14. MONITORING AGENCY NAME & ADDRESS (if different from Controlling Office)	15. SECURITY CLASS. (of this report): UNCLASSIFIED
	15a. DECLASSIFICATION/DOWNGRADING SCHEDULE: N/A

16. DISTRIBUTION STATEMENT (of this Report)

Approved for public release; distribution unlimited.

17. DISTRIBUTION STATEMENT (of the abstract entered in Block 20, if different from Report)

18. SUPPLEMENTARY NOTES

19. KEY WORDS (Continue on reverse side if necessary and identify by block number)

Free Electron Laser (FEL)
tapered wiggler
phase area displacement
sideband instability
gain-expanded FEL

20. ABSTRACT (Continue on reverse side if necessary and identify by block number)

A summary of the Theoretical Studies on Free Electron Lasers and details of the progress for the period October 1, 1982 - September 30, 1983 are presented.

DD FORM 1 JAN 73 1473 EDITION OF 1 NOV 65 IS OBSOLETE

UNCLASSIFIED

SECURITY CLASSIFICATION OF THIS PAGE (When Data Entered)

TABLE OF CONTENTS

THEORETICAL STUDIES ON FREE ELECTRON LASERS

The subject of this investigation has been the Free Electron Laser[1] (FEL), a device which is capable of converting the kinetic energy of a relativistic electron beam into coherent electromagnetic radiation. The investigation focused on two main topics:

A. The FEL operated as an oscillator and an amplifier using variable parameter wigglers.[2]

B. The FEL oscillator operated in conjunction with a storage ring using gain-expanded[3] and phase area displacement wigglers.[2]

During the two-year period extending from August 1, 1981 to September 30, 1983, the following tasks were accomplished:

1. An eigenmode analysis[4] of the linearized one-dimensional FEL equations leading to a determination of the linear gain characteristics of FEL oscillators with variable parameter wigglers. Various cases studied include electron pulses, long and short compared to slippage length; constant and variable parameter wigglers; and FELs with and without optical sideband suppression.

2. The development of a one-dimensional self-consistent particle and electromagnetic wave code[4] to simulate the operation of FELs with variable parameter wigglers and with frequency filtering of the electromagnetic (EM) pulse.

3. A study of the time evolution of an EM pulse in FEL oscillators in which the growth of the pulse is followed from low noise levels all the way to steady state, with particular attention paid to the effectiveness of electron trapping and to the suppression of sideband modes by frequency discrimination.

4. A study of the effect of unstable sideband modes on high-extraction FEL amplifiers, with particular reference to a proposed ATA design.[5]

5. An extension of the analytic linear theory of unstable sideband modes to include not only the amplitude perturbations previously considered,[2] but also the phase perturbations of the EM pulse.

6. A Hamiltonian formulation of the electron equations of motion for the "thin lens" gain-expanded FEL,[6] with derivation of the Manley-Rowe relation and generalized gain-spread theorems.

7. A study of the phase area displacement wiggler, with estimation of the theoretical efficiency possible in storage rings.

8. A preliminary survey of the role of two-dimensional effects on FEL operation.

Tasks 1, 2 and 3 for ultra-short electron micropulses as well as most of Task 6 were completed by the end of the first contract year and are discussed in detail in the 1982 Annual Report.[4]

I. FEL OSCILLATOR

In an FEL oscillator, a variable parameter wiggler is positioned between two mirrors and an EM pulse is reflected repeatedly through the wiggler. Relativistic electron micropulses are injected at periodic intervals so that on each forward pass of the pulse through the wiggler, there is overlap of the EM pulse and the electron micropulse. The pulse grows in amplitude on each forward pass and eventually electrons are trapped in the ponderomotive potential well or "bucket" produced by the combined electromagnetic fields of the wiggler and pulse. At this stage, the pulse continues to grow with enhanced efficiency as the bucket is decelerated down the wiggler and energy extracted from the trapped electrons. A stationary state is reached when the energy extracted from the electrons is balanced by the energy losses.

Tasks 1, 2 and 3 address those issues of the operation of an FEL oscillator which relate to the startup phase, saturation of linear gain with effective electron trapping, and stable propagation of the finite amplitude EM pulse in steady state. The principal results are:

1) Adequate linear gain can be obtained in a variable parameter FEL oscillator sufficient to overcome the losses at

the mirrors and to grow the EM pulse to a large amplitude in a finite number of passes.

2) The linear phase of growth saturates at a high enough level to ensure trapping except for systems which seek to enhance linear gain by use of a long constant parameter section at the front.

3) At high saturation amplitudes, frequency discrimination is required to prevent nonlinear breakup of the EM pulse due to the coupling of unstable sideband modes to the periodic motion of the trapped electrons in the bucket. Qualitative agreement with the theory of sideband instabilities is obtained for the width of the frequency filter required to suppress sideband growth.

4) An FEL oscillator with an EM pulse of one micron wavelength has been simulated. With proper frequency discrimination, the EM pulse was grown from noise to a stable steady state and 30 percent efficiency was achieved.

5) A criterion has been derived (and verified numerically) for the minimum current required to have adequate linear gain as well as frequency discrimination:

$$\langle I \rangle > 1.42 \times 10^5 (1 - r) \frac{\Delta\gamma_r r_o^2 \gamma_r^2}{\gamma_r^2 a_w^2 f} \quad \text{amps},$$

where the electron micropulse was assumed to be ultra-short, $\langle I \rangle$ is the current averaged over a slippage distance, r_o the beam radius, $\Delta\gamma_r$ the change in the resonant energy γ_r

while traversing the wiggler of length L, a_w the dimensionless vector potential amplitude of the wiggler, f the filling factor, and (1 - r) the fractional reduction in amplitude due to energy losses on reflection at the mirrors.

6) The limitation on beam thermal spread is determined more by the need for good linear gain than by that for effective electron trapping.

These results were first obtained in the limit of an ultra-short electron micropulse modeled as a δ-function. Due to computer time limitations, this limit is easier to simulate since the number of particle orbits which must be followed is far fewer than that required to represent a long continuous electron micropulse. This limit is also analytically tractable. However, the basic physics of the electron-photon interaction is qualitatively the same for long electron micropulses. The details of this investigation may be found in the first annual report.

The theory of linear gain for the more realistic limit of long electron micropulses is discussed in Appendix A. Simulations of micropulses several slippage distances long exhibit a behavior similar to that of ultra-short pulses. Because of computer time constraints, only a limited number of simulations of finite length micropulses have been done (up to four slippage distances long). It was again found that frequency discrimination is necessary to suppress the

growth of unstable sidebands. In the absence of frequency discrimination, the EM pulse shape at saturation is broad but very irregular.[7] With frequency discrimination, smooth pulse shapes were obtained, although the saturated pulse energy was somewhat smaller. However, the indications are that with longer micropulses such as those actually envisaged, frequency discrimination would be effective not only in producing smoother saturated pulse shapes, but also relatively higher pulse energies.

The physics of the saturated state should not depend on the electron micropulse length since the EM pulse is many synchrotron bounce periods in length. From arguments similar to those used in the case of the ultra-short pulse, a corresponding minimum current can be derived which ensures that a value of frequency discrimination may be chosen to allow for both linear gain and stable propagation:

$$I_p > 2.77 \times 10^4 (1 - r) (\Delta\gamma_r)^{3/2} \left(\frac{k_w r_o^4}{L^3}\right)^{\frac{1}{2}} \frac{\gamma_r^{3/2}}{a_w^2 f} \text{ amps}$$

I_p is the peak current. Note that the usual resonance condition $k_s = 2k_w\gamma_r^2/(1 + a_w^2)$ applies and that usually the length L is limited by the Rayleigh condition $L < k_s r_o^2$. Details of the derivation are given in Appendix A.

II. FEL AMPLIFIER

In high-gain FEL amplifiers, electrons are trapped in the bucket at the front of the wiggler, the bucket is decelerated and energy is transferred from the trapped electrons to the EM pulse in one pass. Since the trapped electrons undergo many bounce oscillations in the bucket during its passage through the wiggler, the growth of the unstable sideband modes which can detrap electrons and reduce energy extraction efficiency is also a major concern.

In Task 4, a series of simulation runs were carried out using the one-dimensional long pulse simulation code described in Appendix B in order to assess the effect of sideband instabilities on efficiency in the ATA FEL amplifier experiment planned at the Lawrence Livermore National Laboratory (LLNL). A typical set of design parameters for the proposed ATA FEL amplifier is:

Table 1

γ	= 98.85 $\pm$ 1.87		electron beam
I_p	= 5.93 kA		
r_o	= 0.387 cm		
P_{input}	= 2.4 Gigawatts	λ_w	= 8 cm
r_p	= 0.447 cm	A_{ow}	= 3.026 kilogauss-cm
λ_s	= 10.6×10^{-4} cm	$\Delta\gamma_r/\gamma_r$	= 0.33
L	= 22 meters		

$\Delta\gamma_r$ is the effective change in γ_r down the wiggler. The actual wiggler profile is shown in Figure 1.

The results of the simulations using the above parameters are:

1. With zero initial noise perturbation in the EM pulse, an FEL efficiency of 18 percent was observed, agreeing with LLNL estimates. About 54 percent of the electrons were effectively trapped. Figure 2 displays a plot of the dimensionless pulse amplitude as a function of the dimensionless independent variable $v = (t - z/c)\ c/L(c/V-1)$ for $u = (z/V - t)\ c/L(c/V-1) = 0$. Note that $k_w(z) =$ constant. The wiggler extends from $v = 0$ to $v = 1$. The pulse amplitude increases by a factor of 4.8 through the wiggler. Outside the wiggler ($v > 1$), the pulse amplitude is constant.

The bounce frequency ω_B of electron trapped at the bottom of the bucket varied from $\omega_{Bi}k_wL/\omega_s = 61$ at the front of the wiggler to $\omega_{Bf}k_wL/\omega_s = 113$ at the back of the wiggler.

2. With initial perturbations of sideband modes at a frequency ω in the range of the bounce frequency ω_B large sideband amplifications were observed. Figure 3 displays a plot of the variation of pulse amplitude with v for the case where the initial amplitude of the sideband mode at frequency $\omega k_wL/\omega_s = 90$ was 0.001 of the main pulse

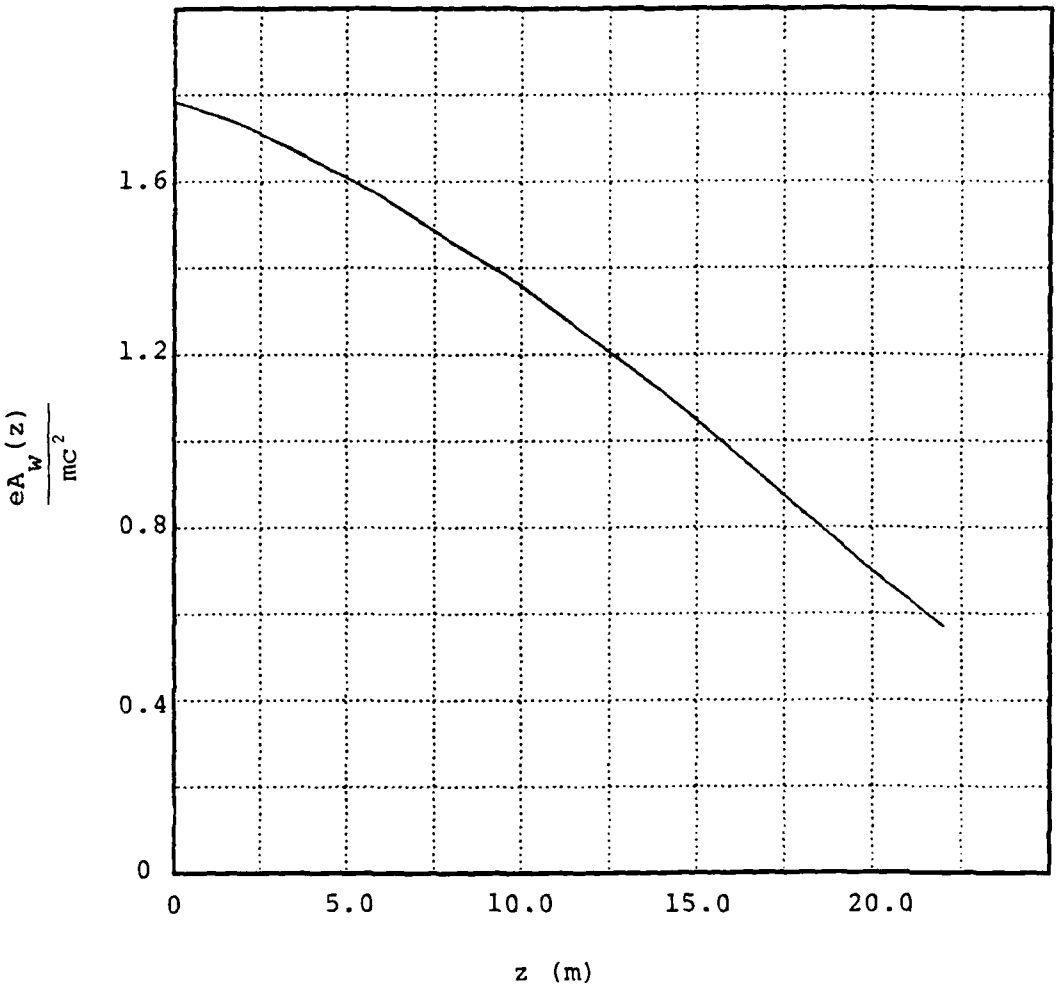

Figure 1. Wiggler vector potential amplitude profile for a simulated FEL amplifier.

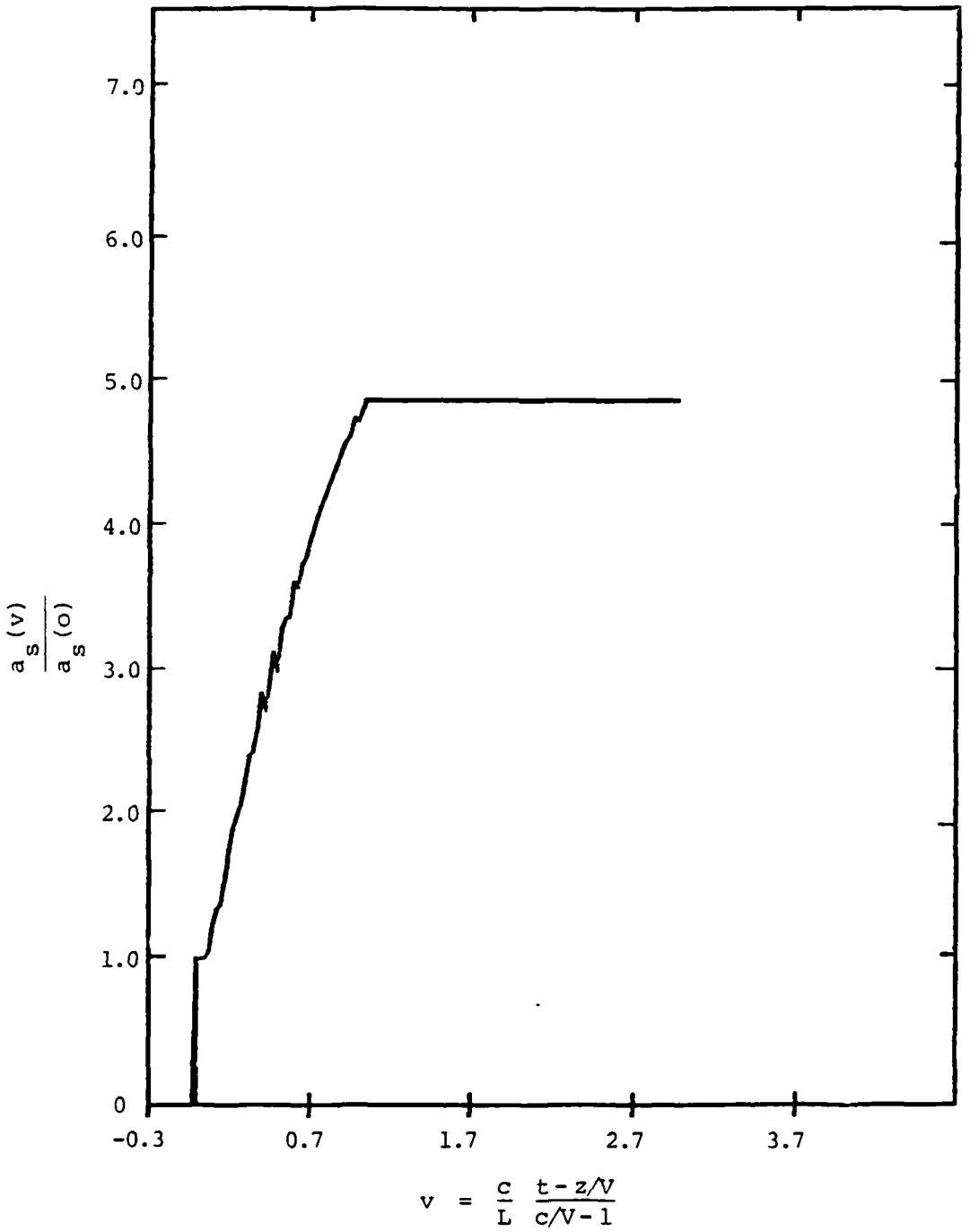

Figure 2. Normalized output optical pulse amplitude profile for a simulated FEL amplifier - no sidebands.

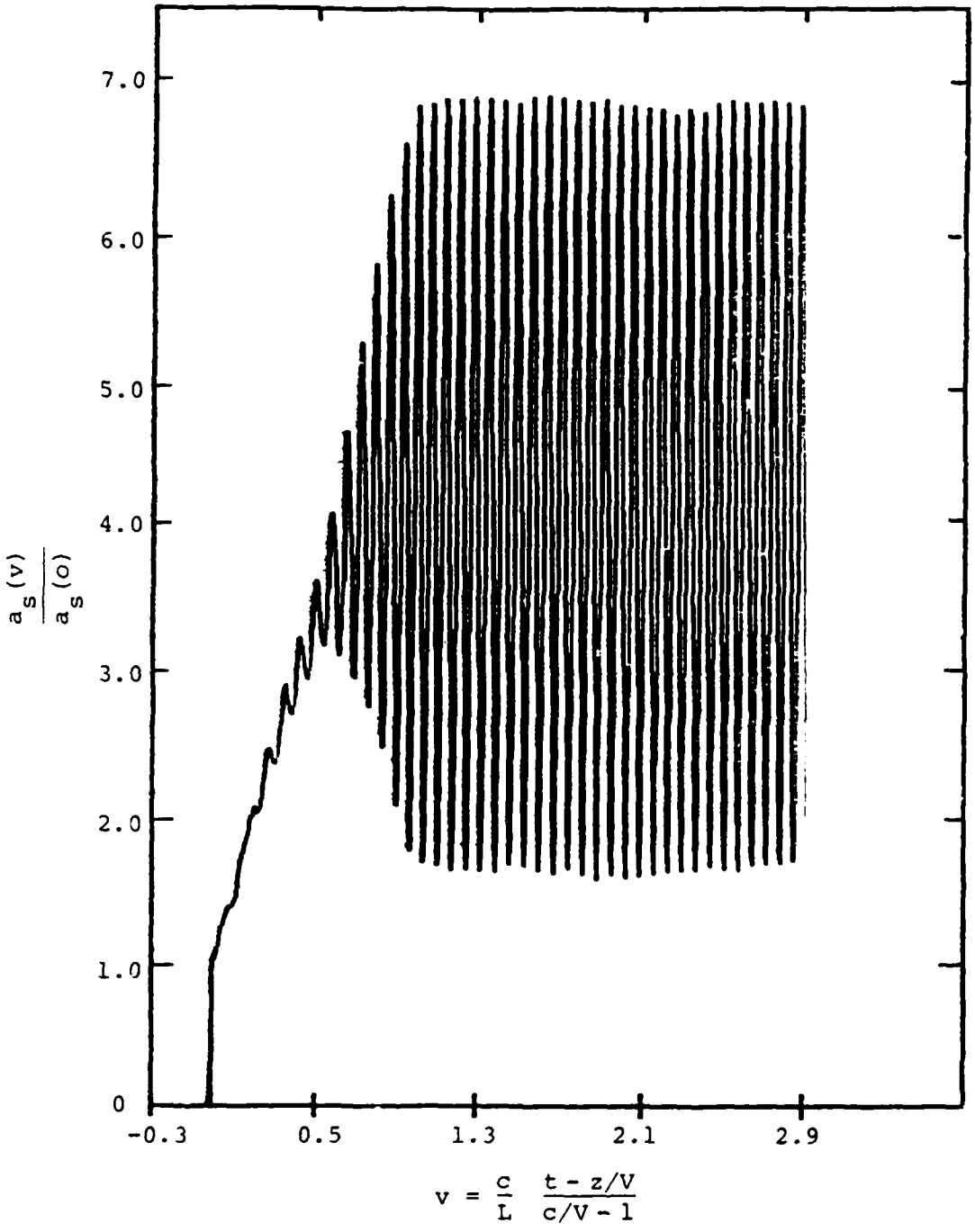

Figure 3. Normalized output optical pulse amplitude profile for a simulated FEL amplifier - 10^{-3} relative initial sideband perturbation at $\omega k_w L/\omega_s = 90$.

amplitude. The sideband mode grew in amplitude by a factor of ~2,660. In Table 2, the amplitude amplification factor of sideband modes is tabulated for different values of frequency $\omega k_w L/\omega_s$.

Table 2

Sideband Frequency ω $k_w L\omega/k_s c$	Ratio of Initial Sideband Amplitude to Main Pulse Amplitude	Amplification Factor
50	10^{-3}	3.7×10^2
90	10^{-3}	26.6×10^2
130	10^{-3}	4.6×10^2
150	10^{-3}	7.7×10^2
165	10^{-3}	5.9×10^2
180	10^{-3}	4.5×10^2

The observed sideband amplification factors are consistent with a theoretical analysis of sideband growth for a high extraction FEL amplifier in which the electrons are all deeply trapped. The details of this analysis will be reported elsewhere.

3. With an initial white noise perturbation containing 0.5% of the optical pulse energy but only about 10^{-4} of the optical pulse energy in the sideband frequency range, the sidebands grew to appreciable amplitudes and the resulting

output pulse shape ($v > 1$) displayed in Figure 4 was highly irregular. The efficiency was reduced from 18% to 15% and the effective trapping from 54% to 44%.

No serious degradation in efficiency occurs until the noise on the incoming laser or e-beam pulse is of order 10^{-4}, well above that due to spontaneous emission. Clearly a 2-D sideband theory is required to assess whether beam quality under circumstances such as shown in Figure 4 is severely degraded.

Since the growth of sidebands in an amplifier is exponential, the growth may be expected to be a sensitive function of detailed design parameters.

While even the large levels of growth predicted here would not be sufficient to amplify spontaneous emission, it is clear that it is essential that noise levels on the electron beam or laser not be excessive. We may note that coherent transverse oscillations of the beam induced by accelerator or transport systems could represent such a noise source. The second and higher harmonics of the betatron frequency are in the dangerous range for sideband growth.

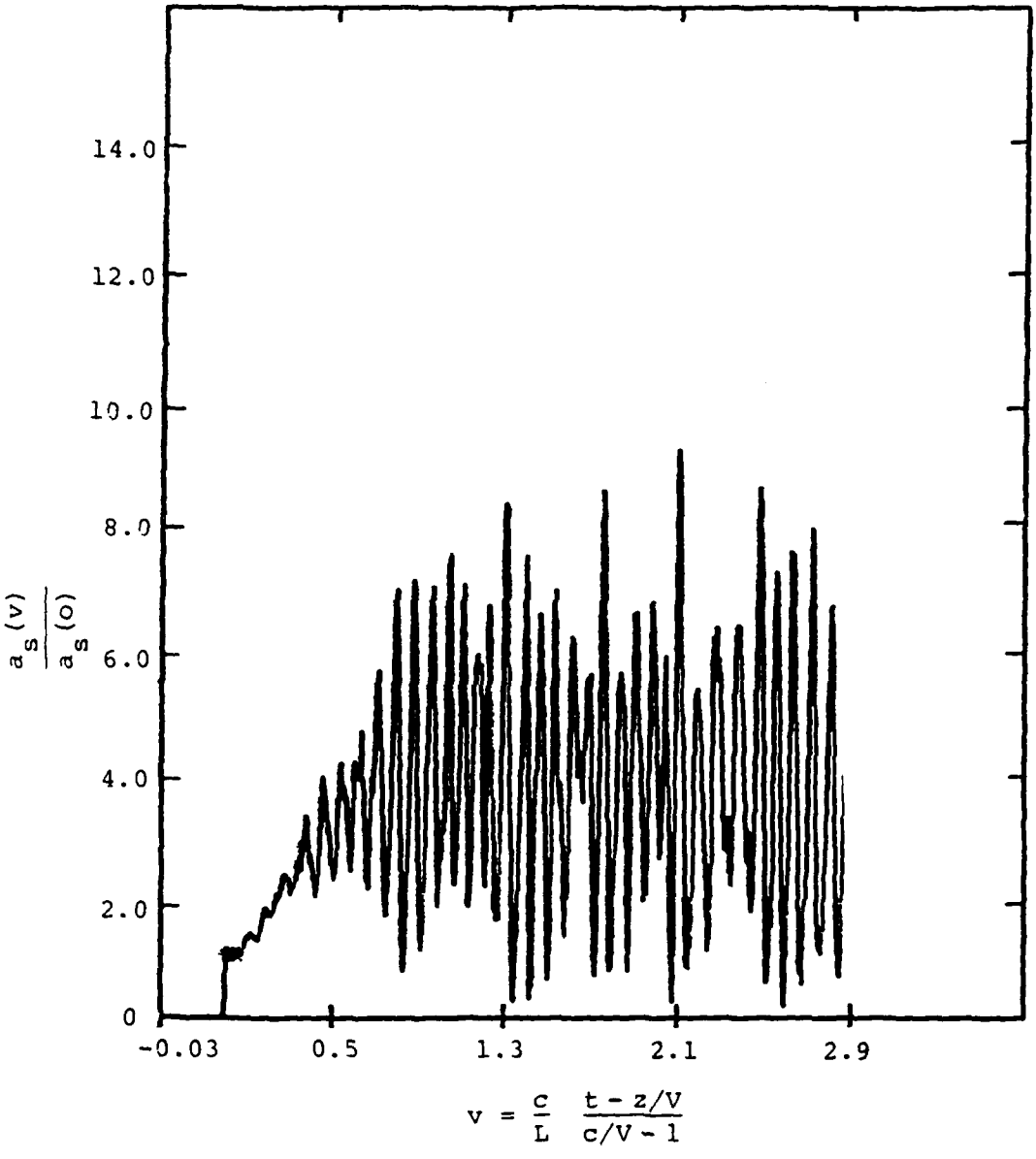

Figure 4. Normalized output optical pulse amplitude profile for a simulated FEL amplifier - 10^{-4} relative initial sideband energy with uniform noise spectrum.

III. SIDEBANDS

One of the principal problems with tapered wiggler oscillators is their instability with respect to sideband growth necessitating frequency discriminatory optics. The previous theory[2] has neglected the effect of the electrons on the optical phase. The theory has now been redone exactly. Some details are presented in Appendix C.

In Figures 5 and 6, the results of analytic theory and simulations for linear growth rates we have done are displayed. Growth of sideband minus growth of signal per pass is plotted in dimensionless units, such that signal growth in these units should be $\sin \psi_r$ (where $\sin \psi_r$ measures the acceleration of the bucket and is defined below in terms of the Hamiltonian), versus sideband frequency κ in units of $(a_0)^{\frac{1}{2}}$, the synchrotron frequency of an electron at the bottom of the ponderomotive well. The growth rates are presented for two particle distribution functions.

(1) Uniformly filled bucket. In Figure 5, linear gain curves for the old and new theories are compared.

While Case (1) is easy to calculate analytically, it is impossible to simulate because of nonlinear effects on particles at the separatrix. Thus we look also at a distribution f_0 with a linear gradient.

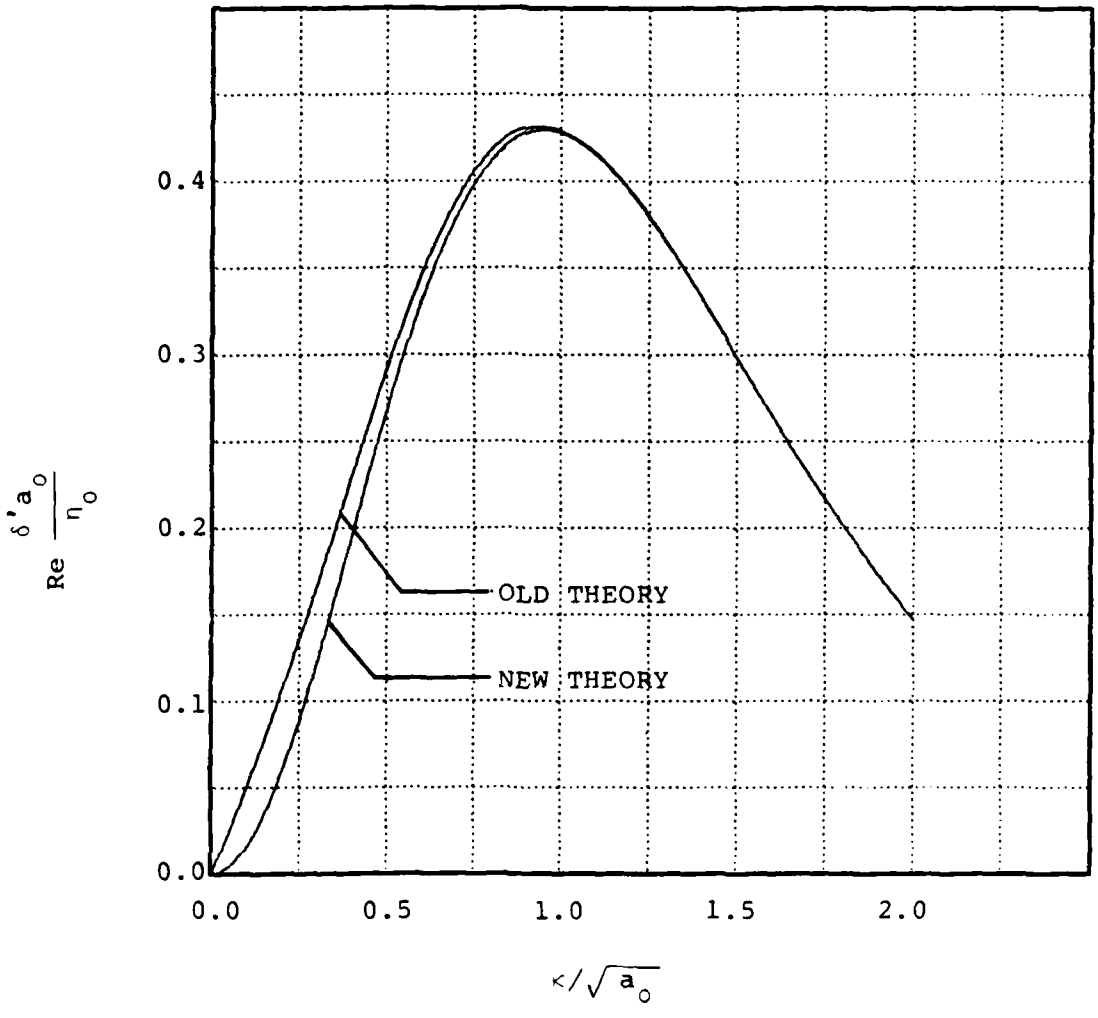

Figure 5. Sideband growth rate - uniformly filled bucket.

$$\delta' \equiv \ell n \left[\left(\frac{a_\kappa(L)}{a_\kappa(o)} \right) \Big/ \left(\frac{a_s(L)}{a_s(o)} \right) \right]$$

$\frac{\eta_o}{a_o}$ is defined in terms of physical parameters in Appendix C.

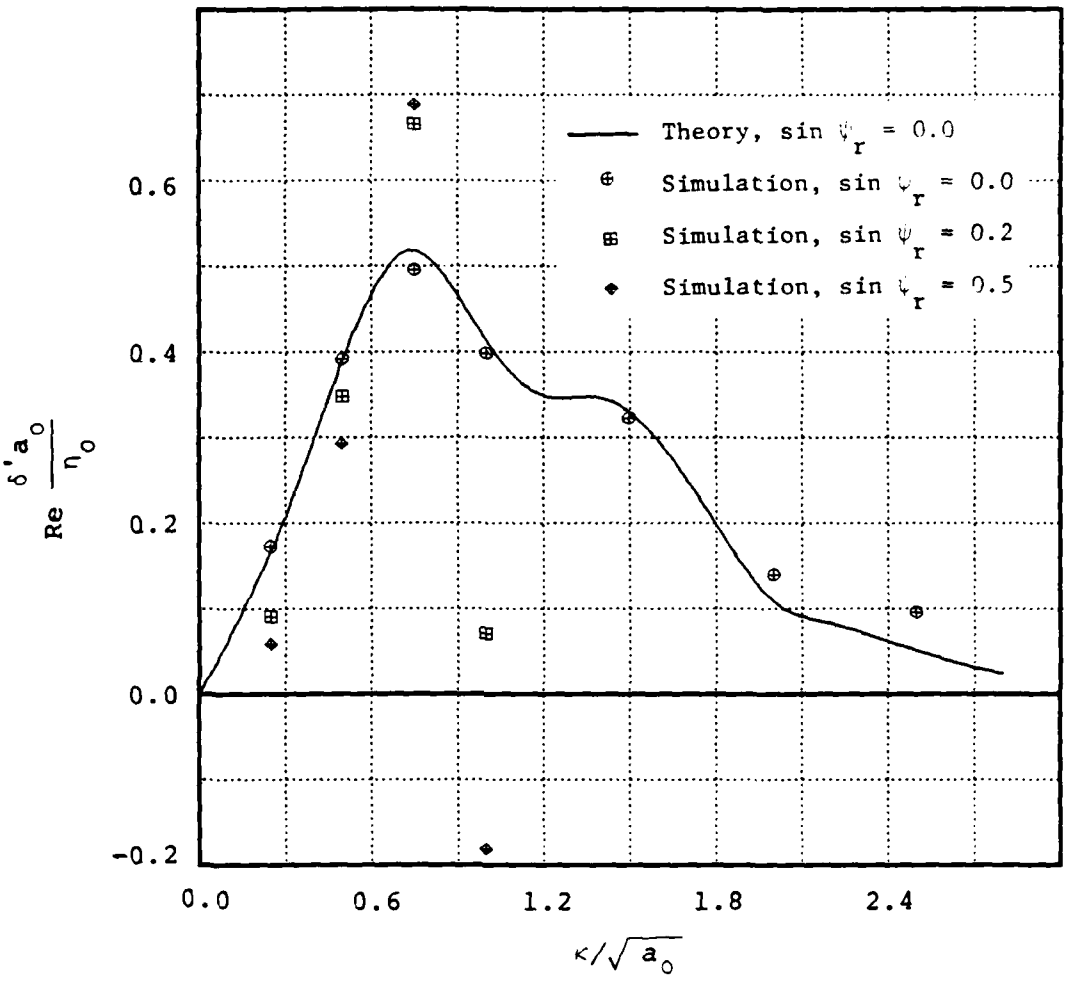

Figure 6. Sideband growth rate - linear weight bucket fill.

$$\delta' \equiv \ell n \left[\left(\frac{a_\kappa(L)}{a_\kappa(o)} \right) \Big/ \left(\frac{a_s(L)}{a_s(o)} \right) \right]$$

$\frac{\eta_o}{a_o}$ is defined in terms of physical parameters in Appendix C.

(2) $f_o = (H_{max} - H)(H_{max} - H_{min})$, where H is the particle Hamiltonian $H = -a_o(\cos\psi + \psi \sin \psi_r)$. The solid curve in Figure 6 is the numerically evaluated analytic dispersion relation for this case with $\sin \psi_r = 0$. It will be observed that for $\sin \psi_r = 0$, the curves for case (1) and case (2) are quite similar so that results may be expected to be prototypical for all distributions which extend over the whole bucket. Sideband growths would be larger for distributions concentrated near the bottom of the bucket.

The points are simulation results for $\sin \psi_r = 0$, 0.2, 0.5. It will be observed that for $\sin \psi_r = 0.2$ and 0.5, the peak growth of sidebands is 4.5 and 2.5, respectively, times signal growth. More detailed comparison between theory and simulation for $\sin \psi_r = 0$ is given in Appendix C.

It should be noted that for $\sin \psi_r \neq 0$, the new theory predicts slightly higher growth than that given in Reference 2. In particular, sideband growth exceeds signal growth at frequencies close to that of the signal, $\delta = 1 + \mathcal{O}(\kappa/\Omega)^2$. Thus, some frequency discrimination is required even against low-lying sidebands.

IV. GAIN-EXPANDED FELs

In a gain-expanded FEL, the sensitivity of gain to variations in the energy of the exciting electrons is reduced by using a periodic magnetic wiggler with transverse gradients such that the electrons which lose energy move to different transverse positions and continue to remain in resonance with the ponderomotive potential well. The reduced sensitivity to energy makes it attractive to operate a gain-expanded FEL in conjunction with a storage ring since many passes of the circulating electrons through the FEL would occur before gain is significantly affected by energy spread. However, transverse betatron oscillations of the electron trajectories are simultaneously excited and may negate the effectiveness of gain expansion unless the oscillation amplitudes are kept small. For steady state operation in a storage ring, it is desirable to maximize the gain while minimizing the level of betatron oscillations.

In order to obtain some insight into the gain characteristics of gain-expanded FELs, a Hamiltonian formulation of the equations of motion for the "thin lens" gain-expanded FEL was derived. Two fundamental limitations on gain-expansion schemes were established: The Manley-Rowe relation which relates gain to betatron excitation, and the generalized Madey theorem relating gain to energy spread and

betatron excitation. The details of this analysis can be found in Appendix A of the 1982 Annual Report.

These analytic results were compared this year with John Madey's Monte Carlo simulation[8] of gain-expanded FELs in storage rings and the following conclusions were reached:

1. The latest version of the simulations are now consistent with the Manley-Rowe and the gain-spread relations.

2. At low laser power, there is good agreement between the simulation and the analytic results. At higher power, the Monte Carlo simulations exhibit some degradation in performance. This may be due to cavity coupling to betatron oscillations which lead to resonance spreading, an effect not included in the analysis. However, proper magnet design which minimizes this coupling could improve the performance.

3. While all designs are limited in consequence of the above theorems to $\Delta E_{laser}/\Delta E_{synchrotron} < \overline{\delta\gamma}/\overline{\gamma}$ where $\overline{\delta\gamma}$ is the rms spread in electron energy, it would appear that gain-expanded wigglers may be advantageous compared to conventional wigglers by virtue of larger energy acceptance. Studies of various designs will continue in collaboration with Madey's group.

V. PHASE AREA DISPLACEMENT

In the deceleration of relativistic beam electrons by a phase area displacement wiggler, the resonant energy of the wiggler is increased from the front to the back such that the bucket is moved through the phase area occupied by the electrons. The result is a downward displacement in the electron energy by an amount of the order of the phase area of the bucket divided by 2π. In the idealized limit of infinitely slow deceleration, there should be no energy spreading.

This method of beam energy extraction has two features which are attractive with respect to operating an FEL oscillator in conjunction with a storage ring: The energy extracted is insensitive to the beam energy spread, and the ratio of the energy extracted to the increase in root mean square energy spread can be made to be small.

Numerical simulations of a one-dimensional FEL with a phase area displacement wiggler have been done and the results were consistent with the theoretical picture of an average energy loss and an average energy spread independent of the initial energy, although the simulated energy loss was about 20 percent lower and the spread about 25 percent higher than predicted by the crude theory. The details of these simulations are described in Appendix D.

An FEL oscillator can be operated in steady state with a storage ring if the laser-induced increase in energy spread can be balanced by a decrease due to incoherent synchrotron radiation and the beam energy boosted by a radio-frequency cavity to compensate for the losses in the wiggler and in synchrotron radiation.

In order to obtain good efficiency during steady state operation, it is essential that the electron interaction with the bucket be adiabatic and that electron trapping be negligible. Typically, adiabaticity requires long wigglers. The bucket must remain essentially constant through the wiggler since bucket variations can affect not only adiabaticity, but lead to electron trapping. Thus, it will be necessary to have a smooth and long (many times the slippage distance) EM pulse, entailing a good frequency discrimination.

If these conditions are satisfied, the FEL efficiency (measured in terms of the ratio of the energy extracted from the electrons $\Delta\gamma_{laser}$ to the energy loss in synchrotron radiation $\Delta\gamma_{syn}$) is estimated to be:

$$\frac{\Delta\gamma_{laser}}{\Delta\gamma_{syn}} \sim 0.05\, k_w^2 L^2 \left(\frac{a_w}{1+a_w^2}\right)^{3/2} \left(\frac{P(GW)}{k_s^2 r_p^2}\right)^{3/4}$$

Here $a_w \sim 1$ is the wiggler dimensionless magnetic vector potential, k_w the wave number, k_s the optical wave number, and r_p the optical pulse radius.

For a particular design discussed in Appendix D, a value of $\Delta\gamma_{laser}/\Delta\gamma_{syn} \sim 0.15$ was observed in the simulation, in rough agreement with theoretical predictions.

Long wigglers containing many wiggler periods and EM pulses with large circulating peak powers are particularly effective in obtaining high efficiencies.

The linear gain per pass tends to be very small unless appreciable micropulse peak current densities are available. Detailed formulae are given in Appendix D. Even if linear gain is adequate, it is not clear whether the desired final steady state is accessible by growing the EM pulse from noise levels. The scenario of the time evolution to a steady state is complex and remains to be elucidated. It is thus not yet clear whether a phase displacement pulse can be grown from noise or whether some alternate startup strategy must be found.

VI. TWO-DIMENSIONAL EFFECTS

Hitherto, the electron equations of motion have been considered as a one-dimensional problem in which the electron motion is reduced to the pendulum equation in the ponderomotive potential well formed by the wiggler and EM pulse fields.

In fact, the electromagnetic fields do depend on transverse dimensions. Transverse variations of the wiggler field produce transverse betatron oscillations and diffraction effects introduce curvature of the wave front.

In the simplest approximation, the transverse betatron oscillation ("frequency" k_β) is decoupled from the longitudinal "synchrotron" oscillation (bounce "frequency" Ω) in the ponderomotive potential well. However, curvature of the wave front couples the two oscillations. This coupling is weak except near resonance when $2k_\beta = \Omega$ which occurs typically at peak circulating power levels near 1 Gigawatt. The details of the effect of this resonance coupling in detrapping electrons is described in Appendix E.

Under resonant conditions, the coupling is marginally strong enough to lead to some detrapping. Thus, a detailed numerical simulation of specific cases may be required.

In an amplifier, it appears that the parameters may change rapidly enough that the resonance is passed through

without significant detrapping. During the buildup phase of an oscillator passing through resonant power levels, the peak potential detrapping is estimated to be of the order of 40 percent if the emittance is the maximum allowed by other considerations. Hence, if a reasonable gain margin exists, this detrapping is not essential. With smaller emittances, the effect is, of course, smaller. For actual cylindrical cases where many orbits do not pass close to the axis, the effect is further reduced.

In the analysis, the self-consistent effect of betatron motion on emission was not studied, but only the effect of an assumed wave shape on electron trapping. Subject to these caveats, it would appears that two-dimensional effects do not seriously perturb the simple one-dimensional picture of an FEL or introduce significant additional design constraints.

ACKNOWLEDGEMENTS

We would like to acknowledge helpful discussions with Norman Kroll and Lee Sloan concerning phase area displacement FEL operation, and with Norman Kroll concerning sideband instability studies. We would also like to acknowledge useful discussions with C. Brau, W. B. Colson, J. C. Goldstein, G. Neil, J. Madey, D. Prosnitz, J. Slater, P. Sprangle and C. M. Tang.

REFERENCES

1. L. R. Elias, W. M. Fairbank, J. M. J. Madey, H. A. Schwettman and T. I. Smith, Phys. Rev. Lett. 35, pp. 717-720 (1976).

   B. E. Newman, R. W. Warren, K. Boyer, J. C. Goldstein, M. C. Whitehead and C. A. Brau, "Optical Gain Results of the Los Alamos Free Electron Laser Amplifier Experiment," Submitted to Society of Photo-Optical Instrumentation Engineers, Special Publication No. 453 (1983 Free Electron Laser Workshop - Orcas Island, WA).

2. N. M. Kroll, P. Morton and M. N. Rosenbluth, "Free Electron Lasers with Variable Parameter Wigglers," IEEE Journal of Quantum Electronics, Vol. QE-17, pp. 1436-1468 (1981).

3. T. I. Smith, J. M. J. Madey, L. R. Elias and D. A. G. Deacon, J. Appl. Phys. 50, 4580 (1979).

   N. M. Kroll, P. L. Morton, M. N. Rosenbluth, J. N. Eckstein and J. M. J. Madey, "Theory of the Transverse Gradient Wiggler," IEEE Journal of Quantum Electronics, Vol. QE-17, pp. 1496-1507 (1981).

4. M. N. Rosenbluth, H. Vernon Wong and B. N. Moore, "Annual Technical Report for Theoretical Studies on Free Electron Lasers," ARA Report No. I-ARA-82-U-89, August 1982.

   M. N. Rosenbluth, H. Vernon Wong and B. N. Moore, "Free Electron Laser (Oscillator) - Linear Gain and Stable Pulse Propagation," Submitted to Society of Photo-Optical Instrumentation Engineers, Special Publication No. 453 (1983 Free Electron Laser Workshop - Orcas Island, WA).

5. D. Prosnitz, A. Szöke and V. K. Neil, "One-Dimensional Computer Simulation of the Variable Wiggler Free Electron Laser," Vol. 7, Free Electron Generators of Coherent Radiation, Addison-Wesley, Reading, MA, pp. 571-587 (1980).

   D. Prosnitz, private communication.

6. M. N. Rosenbluth and H. Vernon Wong, "Annual Technical Report for Theoretical Studies on Free Electron Lasers," Appendix A, ARA Report No. I-ARA-82-U-89, August 1982.

7. John C. Goldstein and W. B. Colson, "Control of Optical Pulse Modulation Due to the Sideband Instability in Free Electron Lasers," Submitted to the Proceedings of the International Conference on Lasers 1982, New Orleans, LA, December 15-17, 1982.

8. J. Madey, private communication.

A P P E N D I X A

THEORY OF LINEAR GAIN: FREE ELECTRON LASERS OPERATED IN OSCILLATOR MODE - FINITE LENGTH ELECTRON PULSE

In the 1982 Annual Report,[1] the theory of linear gain was investigated for a Free Electron Laser (FEL) operated as an oscillator with ultra-short electron pulses. In such a device, a periodic magnetic field wiggler of length L and wave number k_w is positioned between mirrors so that an electromagnetic pulse can be reflected repeatedly through the wiggler. The FEL is driven by a successive series of ultra-short electron beamlets injected at periodic intervals so that there is overlap of beamlet and the electromagnetic pulse on each forward pass through the wiggler. By ultra-short is meant beamlets with length ℓ much less than the slippage distance between electrons and EM pulse $s = k_w L/k_s$, with k_s the wave number of the EM pulse. In fact as we will see herein for the results of Reference 1 to be valid, we must require $s/\Gamma^{k} > \ell > 2\pi/k_s$ with $\Gamma = 2k_w L\ \Delta\gamma_r/\gamma_r >> 1$, where $\Delta\gamma_r/\gamma_r$ is the fractional change in the resonant energy down the wiggler. The linear eigenmode equations, obtained by linearizing the FEL equations in the amplitude of the laser pulse, were analyzed and the linear gain per pass determined as a function of the FEL parameters.

In this paper, we extend the analysis to cover the case of electron beamlets with lengths much larger than the slippage distance, $\ell > s/\Gamma^{\frac{1}{2}}$. Our starting point will be the conventional set of FEL equations applicable in the Compton regime, as derived and discussed in Reference 1. These will be restated without derivation in Section 1 for completeness of presentation.

We anticipate the need to suppress the growth of sideband instabilities when the pulse reaches a finite amplitude sufficient to trap beam electrons. This may be accomplished by frequency discrimination of the pulse in which frequencies above and below the desired pulse frequency ω_s are attenuated. Thus, the analysis will encompass variable parameter wigglers without and with frequency discrimination. The linear eigenmode equation and their solutions are discussed in Section 2 and Section 3 for wigglers without and with frequency discrimination, respectively.

In Section 4, the results are compared with those previously obtained for the ultra-short electron beamlets.

I. FEL Equations

The set of equations which describe the temporal (t) and spatial (z) evolution of the electromagnetic pulse in the wiggler are most conveniently expressed in terms of the new independent variables u and v:

$$u = \frac{c}{L\left(\frac{c}{V} - 1\right)} \left(\frac{z}{V} - t\right)$$

$$v = \frac{c}{L\left(\frac{c}{V} - 1\right)} \left(t - \frac{z}{c}\right)$$

where $V = \omega_s/(k_w+k_s)$ is the electron resonant longitudinal velocity.

The periodic magnetic field wiggler and the electromagnetic pulse are represented by circularly polarized vector potentials $\underline{A}_w$ and $\underline{A}_s$ with negligible spatial variations transverse to the direction of electron beam propagation. The case of plane polarization is given by letting $A \to A/\sqrt{2}$. The electromagnetic pulse is approximated by a plane wave $\sim A_s \exp(-i\omega_s t + ik_s z + i\xi)$ with slowly varying amplitude A_s and phase ξ.

The electron equations of motion are:

$$\frac{\partial \psi}{\partial v} = \hat{\gamma} \tag{1}$$

$$\frac{\partial \hat{\gamma}}{\partial v} = \Gamma + \frac{1}{2}\left[i\hat{a}\, e^{i\psi} - i\hat{a}^* e^{-i\psi}\right] \tag{2}$$

where

$$\hat{\gamma} = \frac{2k_w L}{\gamma_r} (\gamma - \gamma_r)$$

$$\psi = \int_0^z k_w dz + k_s z - \omega_s t$$

$$\gamma_r = \left(\frac{k_s}{2k_w}\right)^{\frac{1}{2}} \left(1 + a_w^2\right)^{\frac{1}{2}}$$

$$\hat{a} = \frac{2k_w k_s L^2}{\gamma_r^2} a_w a_s e^{i\zeta}$$

$$\Gamma = \frac{2k_w L}{\gamma_r} \Delta\gamma_r \quad .$$

γ and ψ are the electron energy and phase angle. $a_w = eA_w/mc^2$ and $a_s = eA_s/mc^2$ are the dimensionless vector potential amplitudes of the magnetic field wiggler and pulse, respectively. $\hat{a}^*$ is the complex conjugate of $\hat{a}$. In these equations, a_w and k_w are considered to be constants, except as they determine the resonant energy γ_r, and the variable parameter wiggler is modeled by $\Gamma \neq 0$, where $\Delta\gamma_r$ corresponds to the change in the resonant energy in going through the wiggler. We are engaged primarily with high efficiency cases, $\Gamma >> 1$. It is also assumed that $\gamma - \gamma_r << \gamma_r$.

The equations for a_s and ζ (from Maxwell's equations) are:

$$\frac{da}{du} = i\eta h(u) \left\langle e^{-i\psi} \right\rangle \tag{3}$$

where

$$\eta = \frac{8\pi e^2 N_T k_w L^2 a_w^2}{\gamma_r mc V(1 + a_w^2)}$$

$$\int du\, h(u) = 1 \quad .$$

N_T is the total number of electrons in the beamlet per unit area, $N_T = \int dz\, n(z,t)$ where $n(z,t)$ is the beam density. $h(u)$ is a form factor which is determined by the profile of the electron beamlet. For an ultra-short pulse as described in Reference 1, $h(u) = \delta(u)$. The angular brackets imply integration over the initial energy distribution and average over the random optical phase of the electrons

$$\left\langle e^{-i\psi} \right\rangle = \frac{1}{2\pi} \int_0^{2\pi} d\psi_0 \int d\hat{\gamma}_0\, f(\hat{\gamma}_0)\, e^{-i\psi}$$

where $f(\hat{\gamma}_0)$ is the initial energy distribution of the electrons.

In u-v space, the wiggler ($L \geq z \geq 0$) lies between the lines $u + v = 0$ and $u + v = 1$. The beam electrons

move on lines of constant u and the photons of the electromagnetic pulse, propagating in the beam direction, move on lines of constant v. The beam electron and photons interact only when their trajectories in the u,v plane intersect within the lines $u + v = 0$ and $u + v = 1$.

II. Linear Theory - Without Frequency Discrimination

The formulation of the linear eigenmode equations has previously been discussed in Reference 1. If we follow the same procedure, we obtain for the pulse amplitude $\hat{a}^n$ on the nth pass:

$$(1 - r + \delta)\ \hat{a}^n - \beta \frac{\partial \hat{a}^n}{\partial v}$$

$$= i\eta \int_{-v}^{1-v} du\, h(u) \left\langle \exp(-i\psi) \right\rangle \tag{4}$$

$$\left\langle \exp\ (-i\psi) \right\rangle$$

$$= \frac{1}{2} \int d\hat{\gamma}_o\, f(\hat{\gamma}_o) \int_{-u}^{v} dv'(v-v')\, \hat{a}^n(v') \tag{5}$$

$$\exp\left\{ i\hat{\gamma}_o (v'-v) + i\frac{(v'+u)^2}{2} - i\frac{(u+v)^2}{2} \right\}$$

r accounts for the reduction in amplitude due to energy losses on reflection at the mirrors and is close to but less than unity. $\beta = k_s C\Delta t/k_w L << 1$ where Δt is the pass-to-pass temporal advance of the electromagnetic pulse relative to the electron beamlet on entry into the wiggler, and $\hat{\gamma}_o$ is the value of $\hat{\gamma}$ at wiggler input. We have expanded $\hat{a}(v+\beta) = \hat{a} + \beta d\hat{a}/dv + \beta^2 \ldots$. The linear gain and phase shift per pass δ is the eigenvalue. The boundary conditions are $\hat{a}^n(v) \to 0$, $v \to \pm \infty$.

In deriving Equation (4) and Equation (5), it is assumed that $\delta << 1$.

Substituting Equation (5) in Equation (4)

$$\beta \frac{\partial \hat{a}}{\partial v} - (1 - r + \delta)\,\hat{a}$$

$$= -i \frac{\eta}{2} \int_0^1 dx \int_x^1 dy\; h(y-v)\,\hat{a}(v-x)\; I(x)\; x$$

$$\exp\left(\frac{i\Gamma x^2}{2} - i\Gamma xy\right) \qquad (6)$$

$$\approx \frac{\eta h(-v)}{2\Gamma} \int_0^1 dx\, \hat{a}(v-x)\, I(x)$$

$$\left\{\exp\left(\frac{i\Gamma x^2}{2} - i\Gamma x\right) - \exp\left(-i\frac{\Gamma x^2}{2}\right)\right\}$$

where

$$I(x) = \int d\hat{\gamma}_o\, f(\hat{\gamma}_o) \exp(-i\hat{\gamma}_o x)$$

and $h(y-v)$ is assumed in accordance with the long-pulse assumption to be a slowly varying function of its argument so that $h(y-v) \approx h(-v) + \ldots$, $1 > y > 0$. Hereafter we drop the superscript n on $\hat{a}^n$.

If we take $h(u)$ to be Lorentzian

$$h(u) = \frac{1}{\pi u_o} \frac{1}{\left[1 + \frac{u^2}{u_o^2}\right]}$$

and we define the Fourier transform $\hat{b}(k)$ of $\hat{a}$:

$$\hat{b}(k) = \int_{-\infty}^{+\infty} dv\, e^{-ikv}\, \hat{a}(v)$$

we obtain from Equation (6):

$$\frac{1}{\pi u_o^2} \frac{\partial^2 \hat{A}(\kappa)}{\partial \kappa^2} - \left(1 + G_1(\kappa)\right)\hat{A}(\kappa) = 0 \qquad (7)$$

where $\kappa = \;\cdot$

$$\hat{A}(\kappa) = \beta\Gamma^{\frac{1}{2}} (i\kappa - \delta_1)\,\hat{b}$$

$$G_1(\kappa) = \frac{\alpha_1}{(i\kappa - \delta_1)} \int_0^{\Gamma^{\frac{1}{2}}} d\xi\; I\left(\frac{\xi}{\Gamma^{\frac{1}{2}}}\right) \exp(-i\kappa\xi) \left\{ \exp\left(-\frac{i\xi^2}{2}\right) - \exp\left(\frac{i\xi^2}{2} - i\Gamma^{\frac{1}{2}}\xi\right) \right\} \tag{8}$$

$$\delta_1 = (1 - r + \delta)/\beta\Gamma^{\frac{1}{2}}$$

$$\alpha_1 = \frac{\eta}{2\pi u_o \beta\Gamma^2} \quad .$$

The parameter u_o is a measure of the length of the pulse (full width at half maximum), $u_o = \ell/L(1-V/c)$, where $L(1-V/c)$ is the "slippage distance."

We see from the dimensionless form of Equation (7) that the long or short pulse approximations depend on whether $\Gamma^{\frac{1}{2}}u_o$ is large or small compared to unity. It may be seen a posteriori that $\Gamma^{\frac{1}{2}}u_o > 1$ justifies our expansion of $h(y-v)$.

If $G_1(\kappa)$ is now expanded about $\kappa = \kappa_c$ where

$$\frac{\partial G_1(\kappa_o)}{\partial \kappa_o} = 0 \quad , \tag{9}$$

Equation (7) may be approximated by:

$$\frac{1}{\Gamma u_o^2} \frac{\partial^2 \hat{A}}{\partial \kappa^2} - \left\{ 1 + G_1(\kappa_o) + \frac{(\kappa-\kappa_o)^2}{2} \frac{\partial^2 G_1}{\partial \kappa_o^2} \right\} \hat{A} = 0 \quad . \tag{10}$$

Furthermore, if

$$1 + G_1(\kappa_o) + \left(\frac{1}{2\Gamma u_o^2} \frac{\partial^2 G_1}{\partial \kappa_o^2} \right)^{\frac{1}{2}} = 0 \quad , \tag{11}$$

Equation (10) will have the solution:

$$\hat{A} = a_o \exp \left[- \frac{(\kappa-\kappa_o)^2}{2} \left(\frac{\Gamma u_o^2}{2} \frac{\partial^2 G_1}{\partial \kappa_o^2} \right)^{\frac{1}{2}} \right]$$

and this guarantees $\hat{a}(v) \to 0$ as $v \to \pm \infty$ provided that

$$\mathrm{Re} \left(\frac{\partial^2 G_1}{\partial \kappa_o^2} \right)^{\frac{1}{2}} > 0 \quad . \tag{12}$$

Equation (9) and Equation (11), subject to Equation (12), constitute the eigenvalue equation which determines δ_1.

If we take $f(\bar{\gamma}_o)$ to be Lorentzian

$$f(\bar{\gamma}_o) = \frac{1}{\pi \bar{\gamma}_{th}} \frac{1}{\left[1+(\bar{\gamma}_o-\bar{\gamma})^2/\bar{\gamma}_{th}^2\right]}$$

we obtain for $I(\xi/\Gamma^{\frac{1}{2}})$:

$$I\left(\frac{\xi}{\Gamma^{\frac{1}{2}}}\right) = e^{-\varepsilon \xi}$$

$$\varepsilon \equiv \left(\bar{\gamma}_{th} + i\bar{\gamma}\right)/\Gamma^{\frac{1}{2}}$$

and in the limit of an infinitely long wiggler where $\Gamma >> 1$, Equation (8) for $G_1(\kappa)$ may be approximated by:

$$G_1(\kappa) = \frac{\alpha_1}{(i-1)(i\kappa-\xi_1)} Z\left(\frac{i\kappa+\varepsilon}{1-i}\right) \qquad (13)$$

where $Z(\theta)$ is the Plasma Dispersion Function

$$Z(\theta) = 2i \exp(-\theta^2) \int_{-\infty}^{i\theta} d\xi \exp(-\xi^2)$$

If we substitute Equation (13) for $G_1(\kappa)$ in Equation (9) and Equation (11), we obtain the eigenvalue equations

$$1 + \frac{\alpha_1}{2i} Z'(\xi_o) + \left[-\frac{\alpha_1}{8\Gamma u_o^2} \frac{Z''(\xi_o)Z'(\xi_o)}{Z(\xi_o)}\right]^{\frac{1}{2}} = 0 \qquad (14)$$

$$\delta_1 = (1-i)\theta_o + \frac{(i-1)Z(\theta_o)}{Z'(\theta_o)} - \varepsilon \qquad (15)$$

where

$$\theta_o \equiv \frac{i\kappa_o + \varepsilon}{1 - i}$$

$$\mathrm{Re}\left[-\alpha_1 \frac{Z''Z'}{Z}\right]^{\frac{1}{2}} > 0 \quad .$$

Equation (14) is solved for θ_o, and substitution of θ_o in Equation (15) yields δ_1 as a function of α_1, Γu_o^2 and ε.

In the limit of $\Gamma u_o^2 \to \infty$ and $\alpha_1 \equiv \eta/2\pi u_o \beta \Gamma^2 >> 1$, we use the asymptotic form of $Z(\theta_o)$ in Equation (14) to determine $\theta_o^2 \approx i\alpha_1/2$, and after substitution in Equation (15), we obtain for the linear gain:

$$(1 - r + \delta) \approx 2\left(\frac{\eta\beta}{2\pi u_o \Gamma}\right)^{\frac{1}{2}} - \left(\bar{\gamma}_{th} + i\bar{\gamma}\right)\beta \quad . \qquad (16)$$

More generally, Equation (14) and Equation (15) are solved numerically and the variation of the dimensionless linear gain

$$\mathrm{Re}\left(\frac{\delta_1+\epsilon}{\alpha_1}\right) = (1 - r + \delta)\ \frac{2\pi u \Gamma^{3/2}}{\eta}$$

is plotted as a function of $1/\alpha_1$ for various values of $\Gamma^{1/2}u_o$ in Figure 1. The linear gain ($\bar{\gamma}_{th} = 0$, $\Gamma^{1/2}u_o \to \infty$) reaches a maximum

$$\mathrm{Re}(1 - r + \delta)_{max} \approx 1.16\ \frac{\eta}{\pi u_o \Gamma^{3/2}}$$

at a value of

$$\frac{2\pi u_o \beta \Gamma^2}{\eta} \approx 3.$$

The curves for $\Gamma^{1/2}u_o = 1,3$ were obtained by numerically integrating Equation (7) subject to the boundary condition $\hat{A}(\kappa) \to 0$, $\kappa \to \pm\infty$.

There also exist additional solutions of Equation (14) and Equation (15) corresponding to eigenmodes with an increasing number of nodes in the amplitude $\hat{a}(v)$. The linear gain for the three "lowest" eigenmodes in the limit of $\Gamma^{1/2}u_o >> 1$ are displayed in Figure 2. It may be seen that for extremely long wigglers these higher modes may grow even when the fundamental is damped.

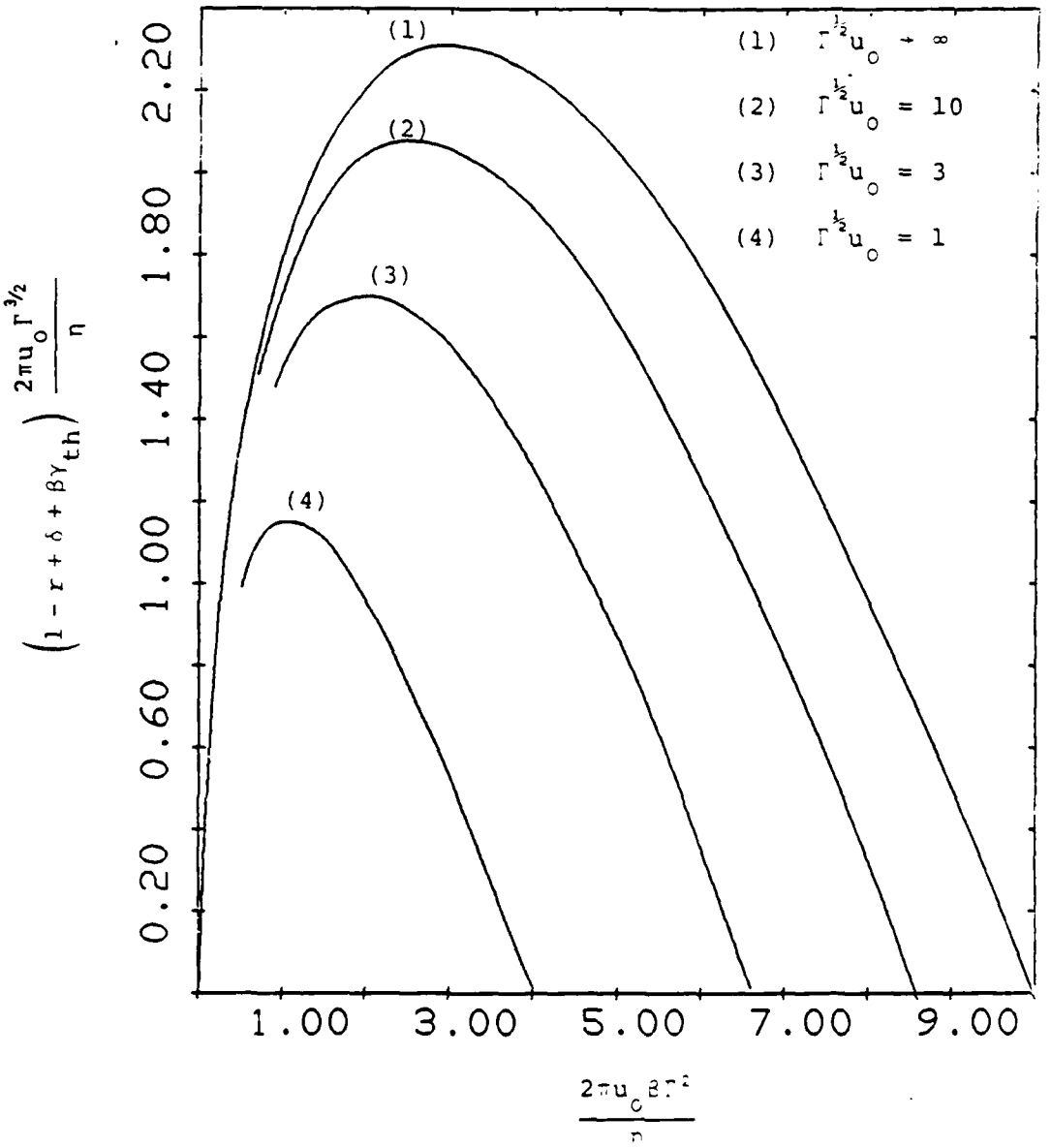

Figure 1. Linear Gain Without Frequency Discrimination

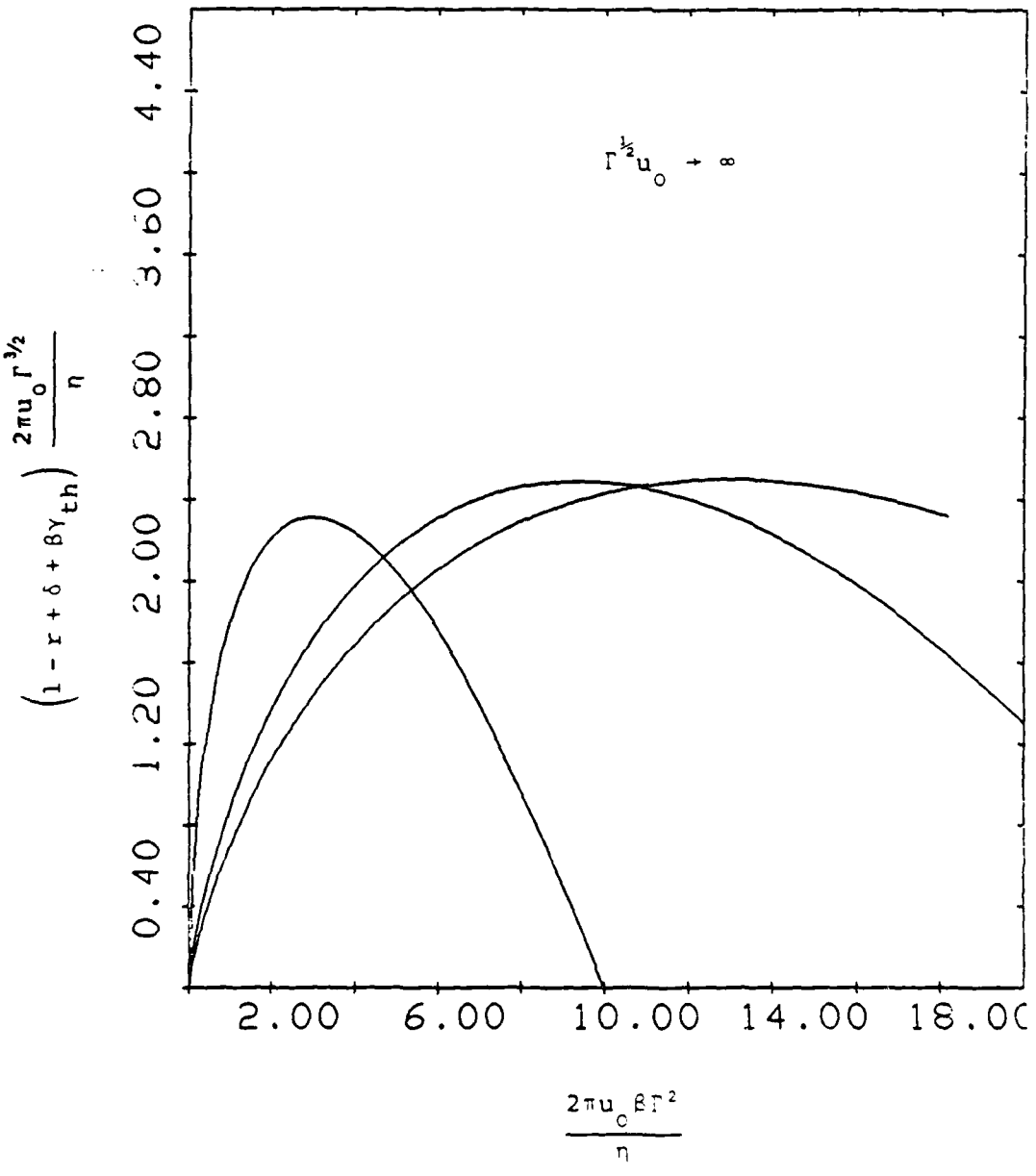

Figure 2. Linear Gain for Three "Lowest" Eigenmodes in the Limit $\Gamma^{1/2} u_o >> 1$

III. Linear Theory - With Frequency Discrimination

With frequency discrimination, the electromagnetic pulse is filtered after each pass through the wiggler by a band pass filter with frequency half width $\Delta\omega$:

$$\Delta\omega = \frac{\nu c}{L(c/V-1)}$$

where ν is an additional parameter which characterizes the magnitude of the frequency half width. Since filtering leads to an effective retardation of the pulse by $1/\nu$ relative to the electron beamlet, while β represents a forward shift, it appears optimal to choose $\nu = 1/\beta$ to avoid the pulse running ahead or lagging behind the electron beamlets.

With this choice of $\nu = 1/\beta$, the linear eigenmode equation for the nth pass is determined by:

$$(1 - r + \delta)\ \hat{a}^n - \frac{\beta^2}{2}\frac{\partial^2 \hat{a}^n}{\partial v^2}$$

$$= i\eta \int_{-v}^{1-v} du\, h(u) \left\langle \exp(-i\ldots) \right\rangle = 0 \qquad (17)$$

A straightforward repetition of the analysis described in Section 2 yields the following equation for the Fourier amplitude $\hat{b}(\kappa)$:

$$\frac{1}{\Gamma u_o^2} \frac{\partial^2}{\partial \kappa^2} \hat{B}(\kappa) - \left(1 - G_2(\kappa)\right) \hat{B}(\kappa) = 0 \tag{18}$$

where

$$k = \Gamma^{1/2} \kappa$$

$$\hat{B}(\kappa) = \frac{\Gamma \beta^2}{2} (\kappa^2 + \delta_2) \hat{b}$$

$$G_2(\kappa) = -\frac{\alpha_2}{(\kappa^2 + \delta_2)} \int_0^{\Gamma^{1/2}} d\xi \; I\left(\frac{\xi}{\Gamma^{1/2}}\right) \exp(-i\kappa\xi)$$

$$\left\{\exp\left(-\frac{i\xi^2}{2}\right) - \exp\left(\frac{i\xi^2}{2} - i\Gamma^{1/2}\xi\right)\right\}$$

$$\alpha_2 = \frac{\eta}{\pi u_o \beta^2 \Gamma^{5/2}} \tag{19}$$

$$\delta_2 = \frac{2(1 - r + \delta)}{\beta^2 \Gamma}$$

Thus, the eigenvalue equations are given by:

$$\frac{\partial G_2(\kappa_o)}{\partial \kappa_o} = 0 \tag{20}$$

$$1 + G_2(\kappa_o) + \left(\frac{1}{2\Gamma u_o^2} \frac{\partial^2 G_2}{\partial \kappa^2}\right)^{1/2} \tag{21}$$

subject to the requirement

$$\mathrm{Re}\left(\frac{\partial^2 G_2}{\partial \kappa_o^2}\right)^{\frac{1}{2}} > 0 \quad . \tag{22}$$

For an initial distribution function $f(\hat{\gamma}_o)$ which is Lorentzian, and in the limit of an infinitely long wiggler where $\Gamma^{\frac{1}{2}} >> 1$, Equation (19) for $G_2(\kappa)$ may be approximated by:

$$G_2(\kappa) = -\frac{\alpha_2 Z\left(\frac{i\kappa+\varepsilon}{1-i}\right)}{(\kappa^2+\varepsilon_2)(i-1)} \quad . \tag{23}$$

If we substitute Equation (23) for $G_2(\kappa)$ in Equation (20) and Equation (21), we obtain:

$$1 - \frac{\alpha_2 Z'(\theta_o)}{4\kappa_o} + \left[\frac{(i-1)\alpha_2 Z'(\theta_o)}{16\Gamma u_o^2 \kappa_o Z(\theta_o)}\left\{\frac{Z'(\theta_o)}{\kappa_o} + \frac{(1-i)}{2} Z''(\theta_o)\right\}\right]^{\frac{1}{2}} = 0 \tag{24}$$

$$\varepsilon = -\kappa_o^2 - \frac{2(1+i)\kappa_o Z(\theta_o)}{Z'(\theta_o)} \tag{25}$$

where

$$\theta_o = \frac{i\kappa_o + \varepsilon}{1 - i}$$

$$\mathrm{Re}\left[\frac{(i-1)\, Z'(\theta_o)}{\kappa_o\, Z(\theta_o)} \left\{\frac{Z'(\theta_o)}{2\kappa_o} + \frac{(1-i)}{4} Z''(\theta_o)\right\}\right]^{1/2} > 0$$

Equation (24) is solved for θ_o, and substitution of θ_o in equation (25) yields δ_2 as a function of α_2, Γu_o^2, and ε.

In the limit of $\Gamma u_o^2 \to \infty$, $\varepsilon \to 0$, and $\alpha_2 \equiv \eta/\pi\, u_o \beta^2 \Gamma^{5/2} >> 1$, we use the asymptotic form of $Z(\theta_o)$ in Equation (24) to determine $\theta_o^3 \approx \alpha_2 (i-1)/8$, and after substitution in Equation (25), we obtain for the linear gain δ:

$$(1 - r + \delta) = \frac{3}{2}\left(\frac{\beta\eta}{2\pi u_o \Gamma}\right)^{2/3} \tag{26}$$

In the limit of $\Gamma u_o^2 \to \infty$, $\varepsilon \to 0$, and $1/\Gamma u_o^2 < \alpha_2 << 1$, we use the series expansion of $Z(\theta_o)$ in Equation (24) and Equation (25) to determine $\theta_o \simeq (1-i)\alpha_2/4$ and the linear gain

$$(1 - r + \delta) = \frac{(1-i)\eta}{4\pi^{1/2} u_o \Gamma^{3/2}} \tag{27}$$

Equation (24) and Equation (25) are solved numerically, and the variation of the dimensionless linear gain

$$\mathrm{Re}(\delta_2/\alpha_2) = \mathrm{Re}\left\{(1 - r + \delta)\,\frac{2\pi u_o \Gamma^{3/2}}{\eta}\right\}$$

is plotted as a function of $1/\alpha_2^{1/2}$ for various values of $\Gamma^{1/2}u_o$ in Figure 3. The linear gain ($\varepsilon=0$, $\Gamma^{1/2}u_o \to \infty$) reaches a maximum

$$\mathrm{Re}(1 - r + \delta) \approx 0.56\,\frac{\eta}{\pi u_o \Gamma^{3/2}}$$

for a value of δ given by

$$\left(\frac{\pi u_o \beta^2 \Gamma^{5/2}}{\eta}\right)^{1/2} \approx 0.81$$

The curves for $\Gamma^{1/2}u_o = 1,3$ were obtained by numerically integrating Equation (18) subject to the boundary condition $\hat{B}(\kappa) \to 0$, $\kappa \to \pm\infty$.

In Figure 4, the reduction in linear gain due to a finite energy spread $\bar{Y}_{th}$ is displayed, while Figure 5 indicates that linear gain is maximized if the input beam energy is below the resonant energy.

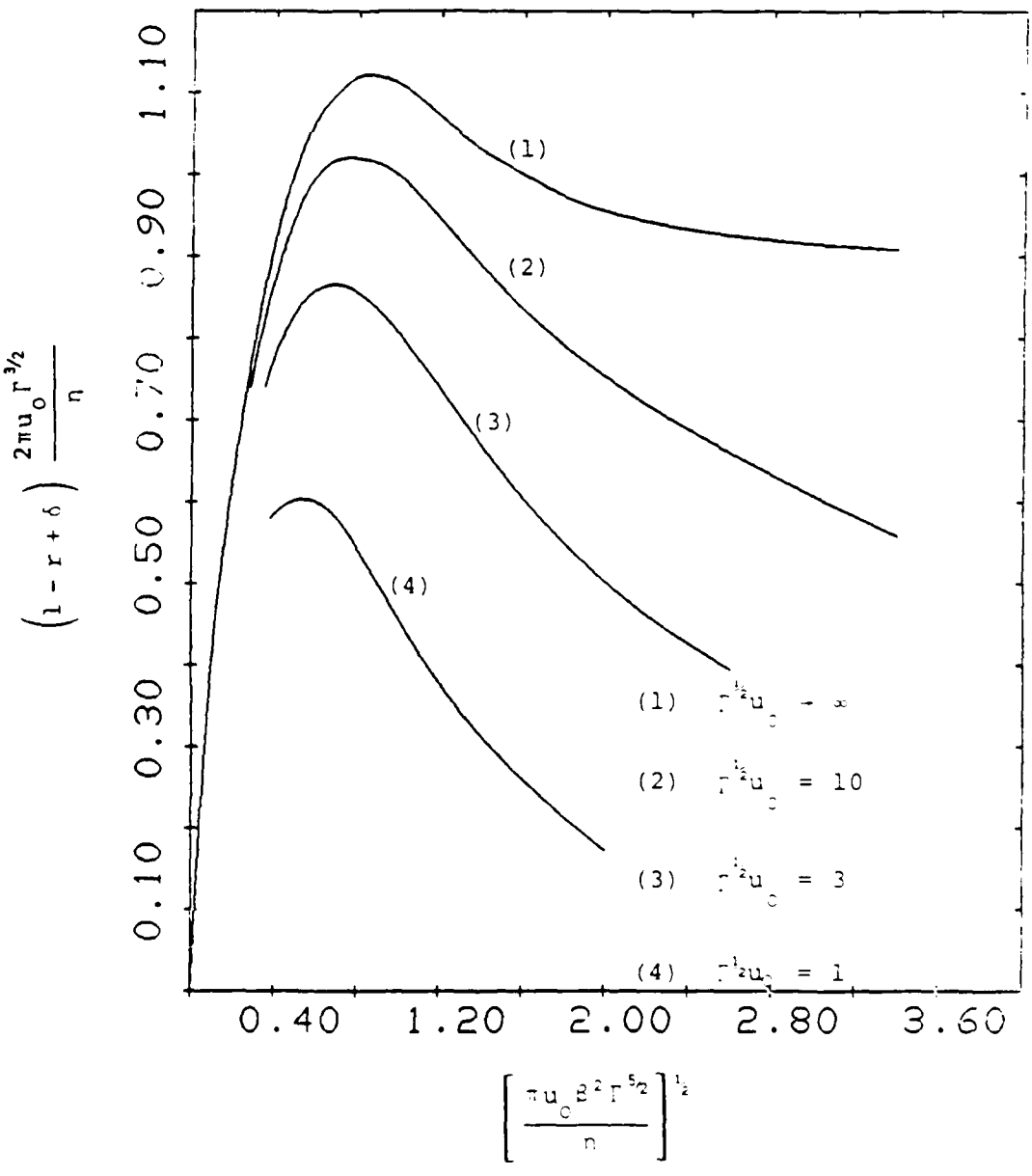

Figure 3. Linear Gain with Frequency Discrimination

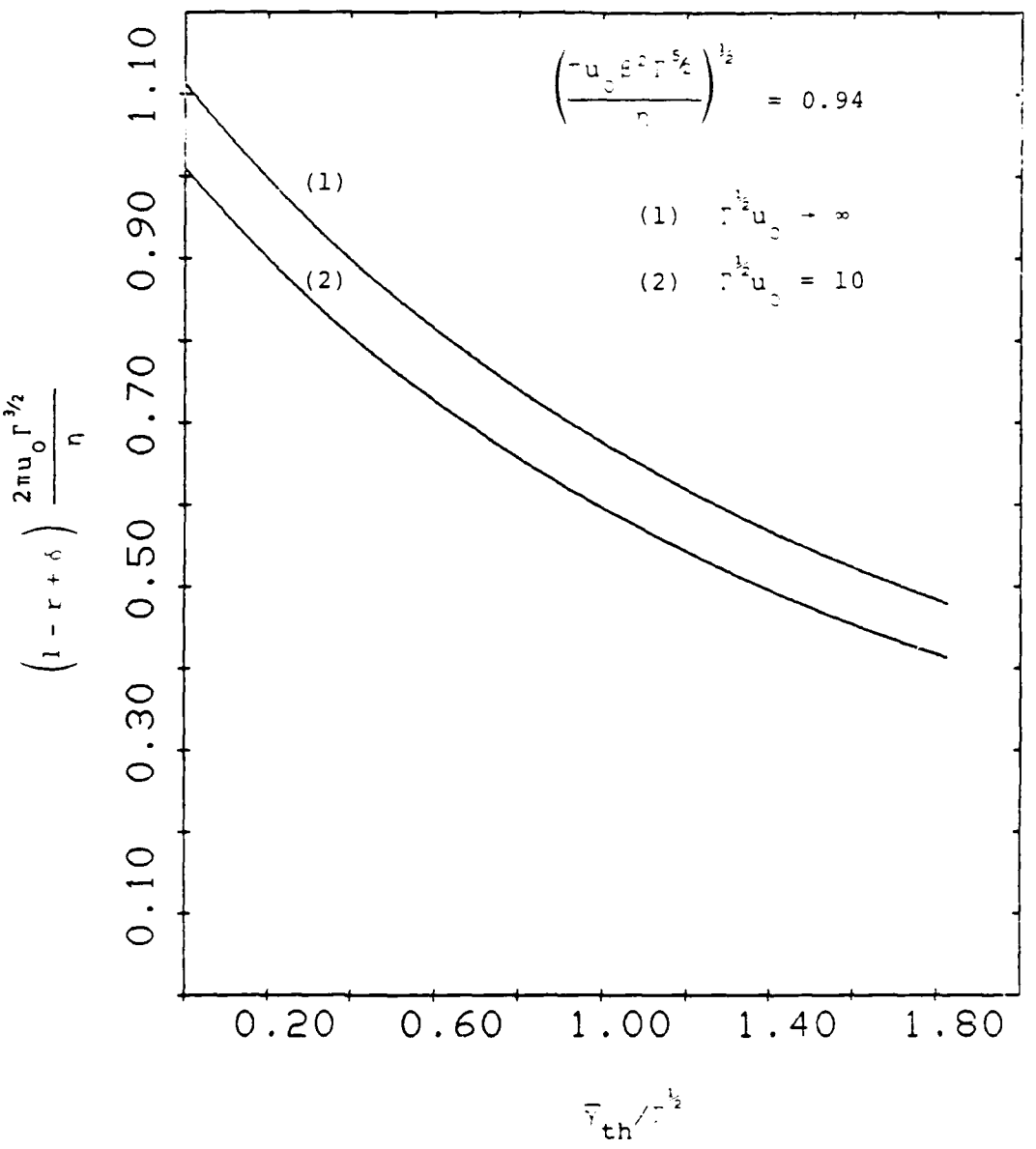

Figure 4. Variation of Linear Gain (Frequency Discrimination) with Energy Spread $\bar{\gamma}_{th}$

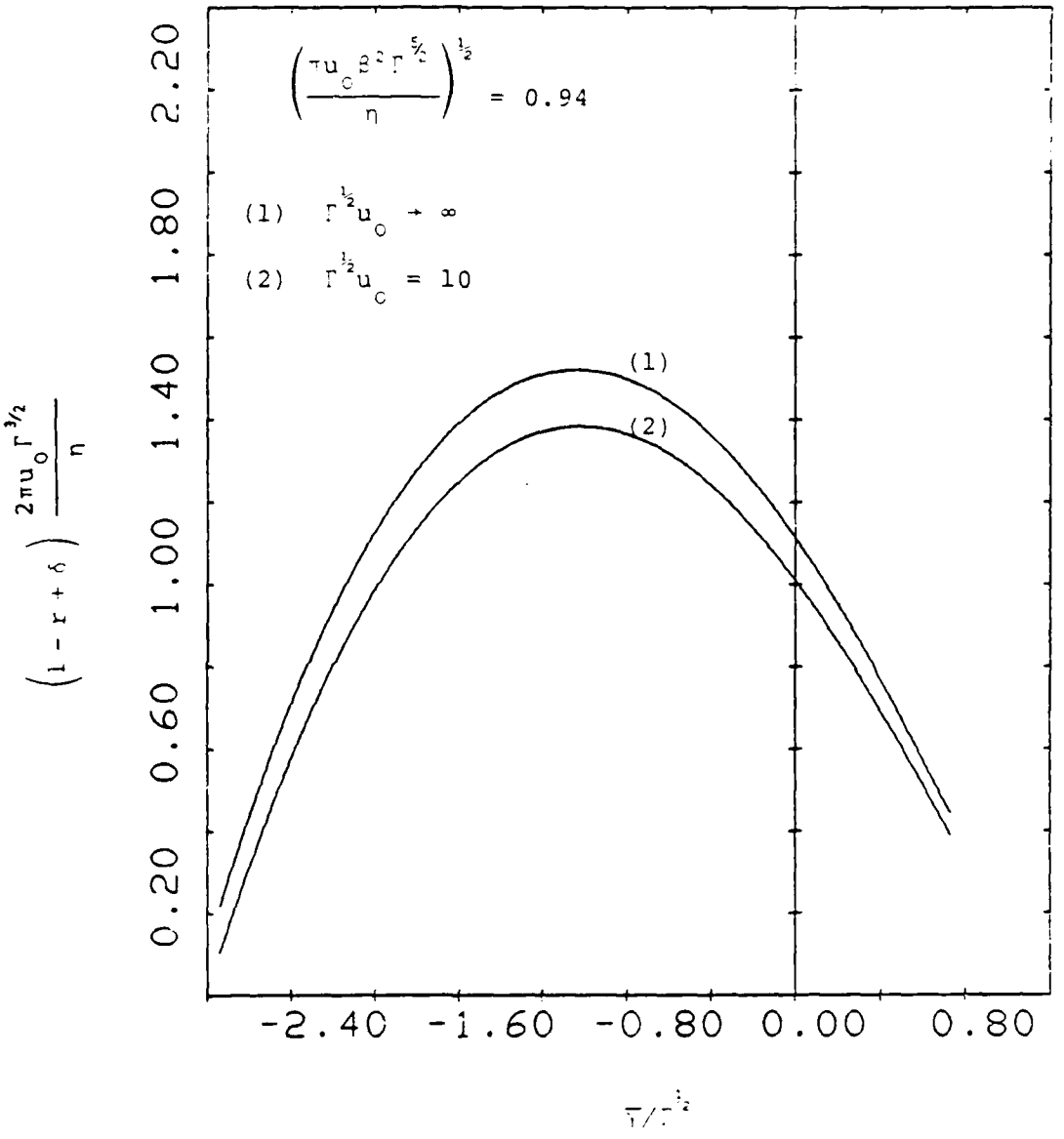

Figure 5. Variation of Linear Gain (Frequency Discrimination) with Mean Energy

Discussion

The long electron beam pulse limit is characterized by

$$\Gamma^{\frac{1}{2}} u_o = \left[2k_w L_w \frac{\Delta\gamma_r}{\gamma_r} \right]^{\frac{1}{2}} u_o >> 1$$

where u_o is the ratio of the pulse length (full width at half maximum) to the slippage distance.

In the limit of a long wiggler ($\Gamma^{\frac{1}{2}} >> 1$) and a long electron beamlet ($\Gamma^{\frac{1}{2}} u_o >> 1$), the linear gain in the absence of frequency discrimination is a maximum

$$\mathrm{Re}(1 - r + \delta)_{max} \approx 1.16 \frac{\eta}{\pi u_o \Gamma^{\frac{3}{2}}}$$

for a value of β given by $[2\pi u_o \beta \Gamma^2/\eta] \approx 3.0$, and it is close to that estimated by Kroll, et al.[2] With frequency discrimination, the linear gain is slightly lower and has a maximum

$$\mathrm{Re}(1 - r + \delta)_{max} \approx 0.56 \frac{\eta}{\pi u_o \Gamma^{\frac{3}{2}}} \quad .$$

for a value of β given by

$$\left[\frac{-u_o \beta^2 \Gamma^{\frac{5}{2}}}{\eta} \right]^{\frac{1}{2}} \approx 0.85$$

The corresponding results of the linear gain[1] analysis for the ultra-short electron beamlet ($\Gamma^{\frac{1}{2}} u_o << 1$) are $Re(1-r+\delta)_{max} \approx .18\eta/\Gamma$ at $2\beta\Gamma^{3/2}/\eta \sim .45$ (without frequency discrimination) and $Re(1-r+\delta)_{max} \approx .105\ \eta/\Gamma$ at $\beta\Gamma/\eta^{\frac{1}{2}} \sim .43$ (with frequency discrimination). Note that for pulse length $\Gamma^{\frac{1}{2}} u_o \sim 1$, the growth rates of long and short pulses are comparable. For longer pulses the growth depends on peak current η/u_o.

Finite temperature reduces gain significantly when $\bar{\gamma}_{th}/\Gamma^{\frac{1}{2}} \geq 1$. Linear gain may be increased somewhat (in the presence of frequency discrimination) if the input beam energy is decreased below the resonant energy.

The need for frequency discrimination to prevent nonlinear breakup of the saturated large amplitude EM pulse due to the growth of sideband instabilities has previously been discussed for the case of ultra-short electron beamlets.[1] It is anticipated that a similar requirement will also be necessary for the case of long electron beamlets.

To suppress sideband frequencies of the order of a quarter of the electron bounce frequency $\sim \frac{1}{2}|\hat{a}|^{\frac{1}{2}}$, the reduction in the pulse energy due to frequency discrimination, that is,

$$|\hat{a}_{\Delta\omega}|^2 \left[1 - \frac{1}{\left(1+\left(\frac{\Delta\omega}{\nu}\right)^2\right)}\right] \sim \left(\frac{\Delta\omega}{\nu}\right)^2 |\hat{a}_{\Delta\omega}|^2 ,$$

should exceed the relative gain due to sideband instabilities. This implies

$$\frac{|\hat{a}|^2}{16\nu^2} > 2(1-r)(\bar{G}-1)$$

where $\bar{G}$ is the ratio of the sideband instability gain to the EM pulse amplitude gain at saturation. If we substitute for the pulse amplitude at saturation

$$|\hat{a}|^2 \frac{\eta\Gamma}{(1-r)\pi u_o}$$

and we take $\nu = 1/\beta$, we obtain

$$\beta^2 \left[\frac{\Gamma\eta}{\pi u_o (1-r)^3}\right]^{\frac{1}{2}} > 32\ (\bar{G}-1)$$

Theoretical estimates[2] indicate $\bar{G} \sim 2$ to 3.

From a survey of the ultra-short electron beamlet simulation results,[3] it was estimated that for stable propagation

$$\beta^2 \left[\frac{\Gamma\eta}{\pi u_o (1-r)^3}\right]^{\frac{1}{2}} \gtrsim 50. \qquad (28)$$

Since the physics of the saturated state does not depend on beam length as the EM pulse is many synchrotron periods in length, this inequality should be applicable to finite length electron beamlets, and stable propagation is obtained by choosing $\beta = 1/\nu$ large enough to satisfy Equation (28).

However, it is also necessary that the choice of β to secure stable propagation be in a parameter regime where the linear gain is finite.

In the limit of a long electron beamlet with no thermal energy spread, the linear gain tends to a non-zero value (Equation 27):

$$\mathrm{Re}(1 - r + \delta) \approx \frac{\eta}{4\pi^{1/2} u_o \Gamma^{3/2}}$$

as β increases,

$$1 >> \frac{\eta}{\pi u_o \beta^2 \Gamma^{5/2}} > \frac{2}{\Gamma u_o^2} \quad .$$

Thus, if we substitute $\beta^2 = \eta u_o / 2\pi\Gamma^{3/2}$ in Equation (28), and we demand $\mathrm{Re}\,\delta > 0$, we obtain the following inequalities to be satisfied in order to have both stable propagation and finite linear gain:

$$\frac{\eta}{\Gamma(1-r)\pi u_o} \geq \frac{21.5}{\Gamma^{1/3} u_o^{4/3}} \tag{29}$$

$$\frac{\eta}{\Gamma(1-r)\pi u_o} > 2.26\,\Gamma^{1/2} \tag{30}$$

These inequalities impose a lower limit on the peak beam current. It should be noted that in deriving these inequalities, a Lorentzian beam profile was considered

$\left(h(u) = 1/\pi u_o\ (1+u^2/u_o^2)\right)$. For $\Gamma^{5/8} u_o > 5.4$, this lower limit is determined by Equation (30), the criterion for finite linear gain. This implies that the peak beam current I_p must exceed a value given by

$$I_p > 9.6 \times 10^3 \left(\frac{\Delta\gamma_r}{\gamma_r}\right)^{3/2} \frac{(1-r)}{k_w r_o} \frac{\left(1+a_w^2\right)^{3/2}}{a_w^2} \text{ amps} \quad (31)$$

where $a_w = eB_w/mk_wc^2$, the wiggler length is $L = k_s r_o^2$, and r_o is the beam radius.

The corresponding inequality for ultra-short beamlets is

$$\frac{\eta}{(1-r)\Gamma} > \frac{I}{0.06} \quad (32)$$

and it may be viewed as an inequality imposing a lower limit on the beam current averaged over a slippage distance.

Equation (30) imposes a current limit comparable to Equation (32) for $\Gamma^{4} \sim 7.4$.

In the proposed Los Alamos FEL experiment $\Gamma^{4} \sim 6$, while for the nominal parameters discussed in Reference 2 $\Gamma^{4} \sim 45$. Thus, Equation (31) implies a required peak beam current for the latter case larger by a factor of ~ 6 than that discussed in Reference (2).

We have not discussed herein the question of transition from linear to saturated states and whether any

difficulty in intermediate states arises from amplitude dependent frequency response, i.e., chirping. This appears best resolved numerically and for the LASL parameters our simulations confirm behavior in linear and saturated states with a smooth transition. Higher efficiency systems (e.g., $\Gamma \approx 1000$) for long beamlets require very lengthy simulations which remain to be done, although for ultra-short beamlets (Reference 3) no new difficulties were observed.

REFERENCES

1. M. N. Rosenbluth, H. Vernon Wong and B. N. Moore, "Annual Technical Report for Theoretical Studies on Free Electron Lasers," ARA Report No. I-ARA-82-U-89, August 1982.

   M. N. Rosenbluth, H. Vernon Wong and B. N. Moore, "Free Electron Laser (Oscillator) - Linear Gain and Stable Pulse Propagation," Submitted to Society of Photo-Optical Instrumentation Engineers, Special Publication No. 453 (1983 Free-Electron Laser Workshop - Orcas Island, WA).

2. N. M. Kroll, P. Morton and M. N. Rosenbluth, "Free Electron Lasers with Variable Parameter Wigglers," IEEE Journal of Quantum Electronics, Vol. QE-17, pp. 1436-1468 (1981).

3. B. N. Moore, M. N. Rosenbluth and H. Vernon Wong, "Simulation of Short Electron Pulse Free Electron Lasers with Variable Parameter Wigglers," ARA Report No. I-ARA-82-U-89, Appendix C, August 1982.

APPENDIX B

SIMULATION ALGORITHM FOR AN ARBITRARILY TAPERED WIGGLER FEL

A relatively simple model of the tapered wiggler FEL has proven adequate for the analysis and simulations involved in determining FEL scaling laws.[1] The crucial simplification involved introduction of a fictitious uniform static electric field into the model. This axial field served to maintain the resonant electrons at a constant γ as energy was extracted by the ponderomotive fields. Thus a uniform wiggler performs as a linearly tapered wiggler.

Recognizing that a more detailed model would be necessary to optimize and evaluate actual tapered wiggler designs, the following model was derived. It has the attractive feature of retaining the basic structure of the simpler one referenced earlier, thus minimizing the recoding necessary to implement it. It differs from the previous model also in that the optical mode is assumed to be a transverse electric rectangular waveguide mode and the wiggler is plane polarized. These added features allow simulation of a larger class of physical designs.

The vector potential for a plane polarized wiggler and transverse electric (TE) optical mode were taken to be

$$A = \hat{x}\, A_w(z) \cos\left(\int_0^z k_w(z)dz \right) - \hat{x}\, A_s(z,t) \cos(k_y y) \cos(k_s z - \omega_s t + \zeta(z,t) \tag{1}$$

Here A_w, k_w, A_s and ζ are the wiggler amplitude and wave number, optical amplitude and phase, and are assumed to be slowly varying functions of their arguments.

Analysis similar to that of Appendix B of Reference 1 yields the following equations for the particle dynamics.

$$\frac{d}{dz}(\gamma - \gamma_r) = -\frac{d\gamma_r}{dz} - \frac{\omega_s a_w a_s}{2\gamma_r c} \sin(\psi + \zeta) \tag{2}$$

$$\frac{d\psi}{dz} = \frac{\omega_s \mu^2}{c\gamma_r^3}(\gamma - \gamma_r) \tag{3}$$

$$\frac{dt}{dz} = (k_w + k_s)\frac{c}{\omega_s} = \frac{1}{c}\left(1 + \frac{\mu^2}{2\gamma_r^2}\right) = \frac{1}{V} \tag{4}$$

where

$$\psi = \int_0^z k_w\, dz + k_s z - \omega_s t \tag{5}$$

$$a_{w,s} = \frac{eA_{w,s}}{mc^2} \tag{6}$$

$$\gamma_r^2 = \frac{\omega_s \mu^2}{2c(k_w + \delta k_s)} \tag{7}$$

$$\mu^2 = 1 + \frac{a_w}{2} \tag{8}$$

$$\delta k_s = k_s - \frac{\omega_s}{c} \tag{9}$$

Averages have been taken over small-scale oscillation and it has been assumed that $\gamma_r^2 >> a_w^2 >> a_s^2$ and $(\gamma-\gamma_r) << \gamma_r$. Also, $\gamma^2 >> 1$ and $\beta_\perp << 1$ prior to entry into the wiggler. All of the particle transverse displacements are assumed negligible compared to $1/k_y$.

The transverse velocity may be computed by assuming conservation of transverse canonical momentum

$$\gamma\beta_x = a_w \cos\left(\int^z k_w dz\right) + \mathcal{O}(a_s, a_w) \tag{10}$$

Making use of the slow variation of a_s and γ, Maxwell's equations

$$\nabla^2 A_x - \frac{1}{c^2}\frac{\partial^2 A_x}{\partial t^2} = -\frac{4\pi}{c} J_x \tag{11}$$

give

$$\left(\frac{\partial}{\partial z} + \frac{\omega_s}{c^2 k_s}\frac{\partial}{\partial t}\right) a_s e^{i\psi} = f \frac{-e^2 a_w}{k_s c m \gamma_r} \left\langle e^{-i\psi} \right\rangle \tag{12}$$

where $H(z/V-t)$ is the electron pulse number density. Note that the effective photon velocity is not c but c^2k_s/ω_s, which is the group velocity of the TE mode. Coupling to other modes has been neglected. The angle brackets represent averages over the particle phase and energy distributions. The filling factor f is defined below and is the result of averages over the $\cos k_y y$ dependence of the TE mode.

Introducing a modified definition of u and v, see Equations (18) and (19) of Appendix C of the 1982 Annual Report,

$$u = \frac{\frac{1}{k_{ow}L}\int_0^z k_w\,dz + \frac{k_s}{k_{ow}L}\,z - \frac{\omega_s t}{k_{ow}L}}{\frac{1}{k_{ow}L}\int_0^L k_w\,dz - \frac{k_y^2}{k_s k_{ow}}} \tag{13}$$

$$v = \frac{\frac{\omega_s t}{k_{ow}L} - \frac{\omega_s^2}{c^2 k_s^2 k_{ow}L}\,z}{\frac{1}{k_{ow}L}\int_0^L k_w\,dz - \frac{k_y^2}{k_s k_{ow}}} \tag{14}$$

Applying this transformation to the equations of motion yields

$$\frac{\partial\gamma}{\partial v} = -\frac{2k_{ow}L}{\gamma_{or}}\frac{\partial\gamma_r}{\partial v} + \frac{\gamma_r}{\gamma}\frac{a_w}{a_{ow}}\frac{q}{2}\frac{i}{2}\left[\dot{a}_s e^{i\cdot} - \dot{a}_s^* e^{-i\cdot}\right] \tag{15}$$

$$\frac{\partial \hat{\gamma}}{\partial v} = \frac{\gamma_{or}}{\gamma_r} \frac{(k_w + k_s)}{k_{ow}} g\hat{\gamma} \tag{16}$$

$$\frac{\partial \hat{a}}{\partial u} = \eta h(u) \frac{a_w}{a_{ow}} \frac{\gamma_{or}}{\gamma_r} g i \left\langle e^{-i\hat{\gamma}} \right\rangle \tag{17}$$

where L is the wiggler length and a_{ow} and k_{ow} are the normalized wiggler vector potential and the wiggler wave number at the input of the wiggler and

$$\hat{\gamma} = 2k_{ow}L \left(\frac{\gamma - \gamma_r}{\gamma_r} \right) \tag{18}$$

$$a = \frac{2k_{ow}L^2}{\gamma_{or}^2} \frac{a_{ow}\omega_s}{c} a_s e^{i\xi} \tag{19}$$

$$g = \frac{\frac{1}{k_{ow}L}\int_0^{L_0} k_w dz - \frac{k_y^2}{k_s k_{ow}}}{\frac{k_w}{k_{ow}} - \frac{k_y^2}{k_s k_{ow}}} \tag{20}$$

$$\eta = \frac{8\pi e^2 L^2 N_T a_{ow}^2 \omega_s}{\gamma_{or} \mu_o^2 k_s mc^2 V} \frac{\left(k_{ow} + k_s\right) f}{\left[\frac{1}{k_{ow}L}\int_0^L k_w dz - \frac{k_y^2}{k_s k_{ow}}\right]} \tag{21}$$

$$f = \frac{2\Delta x_0 \Delta y_0}{y_0 x_0} \quad , \quad \Delta x_0 \Delta y = \text{area of beam} \tag{22}$$

N_T is the total number of electrons per unit area in the beam pulse.

The functions a_w/a_{0w}, k_w/k_{0w}, γ_r/γ_{0r} and y which are known functions of z must be transformed into functions of $u + v$ by the transformation

$$u + v = \frac{\frac{1}{k_{0w}L}\int_0^z k_w\,dz - \frac{k_y^2}{k_s k_{0w}}\,\frac{z}{L}}{\frac{1}{k_{0w}L}\int_0^L k_w\,dz - \frac{k_y^2}{k_s k_{0w}}} \tag{23}$$

Comparing the Equations (15) through (17) with Equations (20) through (22) in Appendix C of Reference 1, it is evident that the algorithms of Equations (26) through (52) of Reference 1, Appendix C may be utilized with the introduction of the functions a_w/a_{0w}, k_w/k_{0w}, γ_r/γ_{0r} and k_y as coefficients.

The diagnostic package was also used intact, but the interpretation of the Fourier transform argument within the wiggler must include the revised transformation from u,v to z,t.

REFERENCE

1. M. N. Rosenbluth, H. Vernon Wong and B. N. Moore, "Annual Technical Report for Theoretical Studies on Free Electron Lasers," Appendix c, ARA Report No. I-ARA-82-U-89, August 1982.

A P P E N D I X C

SIDEBAND INSTABILITIES

The linear theory of sideband instabilities, involving the coupling of small amplitude sideband modes to the periodic motion of electrons trapped in the ponderomotive potential well or "bucket" produced by the combined fields of the wiggler and a large amplitude EM pulse, has previously been discussed neglecting perturbations of the phase of the EM pulse.[1] More recently, the analysis has been extended to include both amplitude and phase perturbations of the EM pulse.

A summary of the principal results will be discussed in this appendix. The details of the analysis will be reported elsewhere.

CONSTANT PARAMETER WIGGLER

We consider stationary states in which the ponderomotive potential well remains constant and is unaccelerated through the wiggler. The EM pulse is represented as a plane wave

---

[1] N. M. Kroll, P. Morton and M. N. Rosenbluth, "Free Electron Lasers with Variable Parameter Wigglers," IEEE Journal of Quantum Electronics, Vol. QE-17, pp. 1436-1468 (1981).

with a slowly varying amplitude A_s and phase ζ_s, $A_s \exp(-i\omega_s t + ik_s z + i\zeta_s)$. The one-dimensional FEL equations, written in terms of dimensionless variables, are described in Appendix A.

The independent coordinates are transformed to Z and v:

$$Z = \frac{z}{L}$$

$$v = \frac{c}{L\left(\frac{c}{V} - 1\right)} \left(t - \frac{z}{c}\right)$$

where L is the wiggler length and V the electron resonant longitudinal velocity. The front of the wiggler is at $Z = 0$ and the back at $Z = 1$.

The linearized FEL equations for the perturbed amplitude $\tilde{A}_s = A_{1s}(Z)\, e^{i\kappa v}$ and phase $\tilde{\zeta}_s = \zeta_1(Z)\, e^{i\kappa v}$ of sideband modes with dimensionless frequency κ are solved to obtain the change in amplitude and phase through the wiggler:

$$\frac{a_1(Z=1) - a_1(0)}{a_o} = \frac{\eta_o}{a_o}\, \zeta_1(0)\, B_{12} \tag{1}$$

$$\zeta_1(Z=1) - \zeta_1(0) = \frac{\eta_o}{a_o^2}\, a_1(0)\, B_{21} \tag{2}$$

where

$$B_{12} = 2\pi \int dJ\, F_o(J) \left(\frac{2E}{K} - 1\right) - I_1(\kappa, \Omega_o) \tag{3}$$

$$B_{21} = -2\pi \int dJ\, F_o(J) \left(\frac{2E}{K} - 1\right) + I_2(\kappa, \Omega_o) \tag{4}$$

$$I_1(\kappa, \Omega_o) = \sum_{n\ \text{odd}} 2\pi\Omega_o \int dJ \frac{\partial F_o}{\partial J} \frac{\pi^4}{K^4} \frac{n^3 q^n}{(1+q^n)^2} g_n(\kappa, \Omega_o) \tag{5}$$

$$I_2(\kappa, \Omega_o) = \sum_{n\ \text{even}} 2\pi\Omega_o \int dJ \frac{\partial F_o}{\partial J} \frac{\pi^4}{K^4} \frac{n^3 q^n}{(1-q^n)^2} g_n(\kappa, \Omega_o) \tag{6}$$

$$g_n(\kappa, \Omega_o) = \frac{\Omega_o}{(\kappa - n\Omega)} \left[1 + \frac{i\{1 - \exp(-i(\kappa - n\Omega))\}}{(\kappa - n\Omega)}\right]$$

$$a_o = \frac{4k_w^2 L^2 a_w a_{os}}{(1 + a_w^2)}$$

$$\eta_o = \frac{8(k_w L)^2}{\gamma_r} \frac{a_w^2}{(1+a_w^2)} \frac{L}{k_s r_o^2} f \frac{eI}{mc^3}$$

$$\gamma_r^2 = \frac{k_s}{2k_w} (1 + a_w^2)$$

$$\Omega = \frac{\pi}{2K} \Omega_o$$

$$\Omega_o = a_o^{\frac{1}{2}}$$

$$a_o = \frac{4k_w^2 L^2 a_w a_{os}}{(1 + a_w^2)}$$

$$a_w = \frac{eA_w}{mc^2}$$

$$a_{os} = \frac{eA_{os}}{mc^2}$$

$$J = \frac{8\Omega_o}{\pi} \left\{ E(k) - (1 - k^2) \; K(k) \right\}$$

$$K = \int_0^{\pi/2} \frac{d\xi}{(1 - k^2 \sin^2 \xi)^{\frac{1}{2}}}$$

$$E = \int_0^{\pi/2} d\xi \; (1 - k^2 \sin^2 \xi)^{\frac{1}{2}}$$

$$q = \exp \left\{ - \pi \, K(k') / K(k) \right\}$$

$$k' = (1 - k^2)^{\frac{1}{2}}$$

$$2\pi \int dJ \, F_o(J) = 1 \qquad (7)$$

a_o is the dimensionless amplitude of the finite amplitude pulse and is independent of Z. $a_1(Z)$ is the dimensionless perturbed amplitude. η_o is proportional to the current density $I/\pi r_o^2$, with r_o the beam radius. f is the filling factor. Ω_o is the dimensionless frequency of oscillation at the bottom of the bucket. $F_o(J)$ is the equilibrium distribution function of the electrons trapped in the bucket and is a function of the electron action variable J only. Equation (7) determines the parameter k as a function of J or vice versa. For

electrons at the bottom of the bucket $k \to 0$, $J \to 0$, while at the top $k \to 1$, $J \to \frac{8\Omega_o}{\pi}$.

It is assumed that $\eta_o/a_o << 1$ so that the linear gain per pass is small.

Let $a_1(Z=1) = e^{\delta} a_1(0) = (1 + \delta + \ldots) a_1(0)$, and $\zeta_1(Z=1) = (1 + \delta + \ldots) \zeta_1(0)$ where δ is the linear gain and phase shift per pass. The linear gain δ is determined by substitution in Equations (1) and (2):

$$\delta^2 = \frac{\eta_o^2}{a_o^2} \left[2\pi \int dJ\, F_o(J) \left(\frac{2E}{K} - 1 \right) - I_1 \right] \left[- 2\pi \int dJ\, F_o(J) \left(\frac{2E}{K} - 1 \right) + I_2 \right] \tag{8}$$

If the bounce frequency is large, $\Omega_o >> 1$, g_n may be approximated by $g_n = \Omega_o/(\kappa - n\Omega)$, and I_1 and I_2 reduces to

$$I_1 = \sum_{n\ \mathrm{odd}} 2\pi\, \Omega_o \int dJ\, \frac{\partial F_o}{\partial J}\, \frac{\pi^4}{K^4}\, \frac{n^3 q^n}{(1+q^n)^2}\, \frac{\Omega_o}{(\kappa - n\Omega)} \tag{9}$$

$$I_2 = \sum_{n\ \mathrm{even}} 2\pi\, \Omega_o \int dJ\, \frac{\partial F_o}{\partial J}\, \frac{\pi^4}{K^4}\, \frac{n^3 q^n}{(1-q^n)^2}\, \frac{\Omega_o}{(\kappa - n\Omega)} \tag{10}$$

In the limit of $\kappa >> \Omega_o$, $1/(\kappa - n\Omega)$ may be expanded as a power series in $\kappa/n\Omega$, and by doing the summation in n:

$$I_1 = 2\pi \int dJ\, F_o \left(\frac{2E}{K} - 1\right) + \frac{\kappa^2}{\Omega_o^2} + O\left(\frac{\kappa^4}{\Omega_o^4}\right) \qquad (11)$$

$$I_2 = -\frac{16\Omega_o}{3} \int dJ\, \frac{\partial F_o}{\partial J} \left\{ 2E(2 - k^2) - \frac{3E^2}{K} - k'^2 K \right\} + O\left(\frac{\kappa^2}{\Omega_o^2}\right) \qquad (12)$$

The linear gain δ is then given by:

$$\delta^2 = \frac{\eta_o^2}{a_o^2} \frac{\kappa^2}{\Omega_o^2} \left[2\pi \int dJ\, F_o(J) \left(\frac{E}{K} - 1\right) + \frac{16\Omega_o}{3} \int dJ\, \frac{\partial F_o}{\partial J} \left\{ 2E(2 - k^2) - \frac{3E^2}{K} - k'^2 K \right\} \right] \qquad (13)$$

The magnitude of the linear gain depends on the structure of the electron distribution function $F_o(J)$.

Two specific electron distribution functions have been investigated and the linear gain evaluated as a function of the sideband frequency κ/Ω_o.

Case I

In the case where the bucket is full:

$$F_o = \frac{1}{16\Omega_o}, \quad J < J_{max} = \frac{8\Omega_o}{\pi} \quad . \qquad (14)$$

The integral

$$2\pi \int_0^{J_{max}} dJ\, F_0\left(\frac{2e}{K} - 1\right) = \frac{1}{3}$$

and the summation in Equations (9) and (10) for I_1 and I_2 ($\Omega_0 >> 1$ is assumed to be large) may be converted into an integral:

$$I_1 = -\sum_{n \text{ odd}} \frac{\pi}{8} \left[\frac{\pi^4}{K^4} \frac{n^3 q^n}{(1+q^n)^2} \frac{\Omega_0}{(\kappa - n\Omega)} \right]_{k^2 \to 1}$$

$$= -\frac{2}{\pi^2} \int_{-\infty}^{+\infty} d\lambda \frac{\lambda^3}{\cosh^2 \lambda} \frac{1}{(\rho - \lambda)}$$

$$I_2 = -\sum_{n \text{ even}} \frac{\pi}{8} \left[\frac{\pi^2}{K^4} \frac{n^3 q^n}{(1-q^n)^2} \frac{\Omega_0}{(\kappa - n\Omega)} \right]_{k^2 \to 1}$$

$$= -\frac{2}{\pi^2} \int_{-\infty}^{+\infty} d\lambda \frac{\lambda^3}{\sinh^2 \lambda} \frac{1}{(\rho - \lambda)}$$

where $\rho = \frac{\pi\kappa}{2\Omega_0}$.

The integrals may be written in terms of ψ-functions or an infinite sum. The linear gain δ is then determined by:

$$\delta^2 = \left(\frac{\eta}{a_o}\right)^2 \left[\frac{2\pi^2 y^3}{\sinh^2 \pi y} + i\left(\frac{1}{3} - 4y^2 + 8y^4 \sum_{n=0}^{\infty} \frac{n+1}{\left|(n+1)^2 + y^2\right|^2}\right)\right]$$

$$\left[\frac{2\pi^2 y^3}{\cosh^2 \pi y} + i\left(4y^2 - 8y^4 \sum_{n=0}^{\infty} \frac{n+\frac{1}{2}}{\left|(n+\frac{1}{2})^2 + y^2\right|^2}\right)\right] \qquad (15)$$

where $y = \frac{\rho}{\pi} = \frac{\kappa}{2\Omega_o}$.

$\mathrm{Re}\ \frac{\delta a_o}{\eta_o}$ is tabulated as a function of $\frac{\kappa}{\Omega_o}$ in Table 1.

Table 1

$\frac{\kappa}{\Omega_o}$	$\mathrm{Re}\ \frac{\delta a_o}{\eta_o}$
0.2	0.059
0.4	0.196
0.6	0.332
0.8	0.412
1.0	0.428
1.2	0.393
1.6	0.265
2.0	0.147

No comparison with simulations has been made because of the anticipated difficulty (imposed by running time limitations) in having adequate numbers of particles very close to the separatrix, $k^2 \to 1$.

Case II

In the case where F_o decreases linearly in k^2 from the bottom to the top of the bucket

$$F = \frac{9}{64\Omega_o}(1 - k^2), \quad 1 > k^2 > 0 \quad , \tag{16}$$

the integrals in J may be transformed to integrals in k^2, $\int dJ \to \int dk^2 \frac{4\Omega_o K}{\pi}$. Thus $2\pi \int dJ F_o(J) \left(\frac{2E}{K} - 1\right) = 0.6$, and the other integrals may be evaluated numerically. In the limit $\frac{\kappa^2}{\Omega_o^2} << 1$, Equation (13) yields for the linear gain:

$$\delta = 0.62 \frac{\eta_o}{a_o} \frac{\kappa}{\Omega_o} \quad . \tag{17}$$

More generally, using Equations (5) and (6) for I and I_2, the linear gain δ may be calculated from Equation (8). Ten terms in each sum $10 > n > -10$ are sufficient to obtain convergence. $\mathrm{Re}\,\delta$ is tabulated in Table 1 for different values of κ/Ω_o. The values of the FEL dimensionless parameters are $\eta_o = 320$ and $a_o = 640$, with $\Omega_o = 25.3$ corresponding to four bounce periods for an electron at the bottom of the bucket.

The linear gain increases linearly with κ/Ω_0 for $\kappa/\Omega_0 << 1$ and reaches a maximum of $\mathrm{Re}\,\delta \approx 0.26$ at $\kappa/\Omega_0 = 0.75$.

The growth of sideband modes has been simulated numerically using our previously-described I-D particle-pushing code.

The electrons are randomly distributed within the trapped region of phase space, weighted by a linear function of k^2 to model the distribution function described by Equation (16). The procedure for determination of the sideband eigenmodes involves three simulation runs, one reference run with only the main optical pulse and two runs with additional linearly-independent perturbations. A response matrix analogous to Equations (1) and (2) is determined by Fourier transforming the output optical pulse and the eigenvalue of this matrix yields the sideband growth rates.

The linear gain evaluated from the simulations are also tabulated in Table 2 for different values of κ/Ω_0.

The agreement between theory and simulations is satisfactory.

The two cases discussed in this appendix are representative of the classes of trapped electron distribution functions which could be found in realistic FELs. It may be noted that the magnitude of the linear gain of

Table 2

$\frac{\kappa}{\Omega_o}$	B_{12}		B_{21}		$\mathrm{Re}\,\frac{\delta a_o}{\eta_o}$	
	SIMULATION	THEORY	SIMULATION	THEORY	SIMULATION	THEORY
0.25	-0.0783 +i 0.0171	-0.0727 +i 0.0281	-0.378 -i 0.0023	-0.380 -i 0.0028	0.173	0.169
0.50	-0.425 +i 0.230	-0.397 +i 0.266	-0.336 +i 0.00776	-0.347 -i 0.00921	0.392	0.391
0.75	- 0.288 +i 1.37	- 0.192 +i 1.46	- 0.260 -i 0.0358	-i 0.273 -i 0.0518	0.496	0.518
1.0	1.45 +i 0.843	1.54 +i 0.752	- 0.166 -i 0.177	- 0.208 -i 0.208	0.398	0.413
1.5	0.702 +i 0.0767	0.725 i 0.102	-0.513 -i 0.543	-0.610 -i 0.552	0.323	0.329
2.0	0.640 +i 0.164	0.702 +i 0.138	-0.798 -i 0.110	-0.833 -i 0.075	0.140	0.109
2.5	0.688 +i 0.113	0.731 +i 0.0645	-0.665 -i 0.0796	-0.701 -i 0.0383	0.096	0.0511

sideband modes as well as the structure of the linear gain dependence on frequency for these two cases are similar.

This analysis can readily be extended to discuss the growth of sideband modes in variable parameter wigglers and is currently in progress. Some preliminary results are presented in Figure 6 of the main summary of this report.

A P P E N D I X D

PHASE AREA DISPLACEMENT

I. INTRODUCTION

In the deceleration of relativistic beam electrons by phase area displacement,[1] the beam electrons are injected into a variable parameter wiggler in which the resonant energy of the wiggler γ_r increases from the front of the wiggler to the back, $\gamma_r(L) > \gamma_r(0)$. The beam energy γ is such as to produce a resonant interaction of the beam electrons with the ponderomotive potential well or "bucket" (produced by the combined fields of the wiggler and electromagnetic [EM] pulse) inside the wiggler, $\gamma = \gamma_r(z)$, $L > z > 0$, usually near the center of the wiggler. The interaction may be viewed, as shown in Figure 1, in terms of an acceleration of the bucket through the phase area (γ,ψ) of the beam electrons. The result is a downward displacement in energy of the phase area occupied by the beam electrons by an amount of the order of the phase area of the bucket divided by 2π.

If the bucket acceleration is adiabatic and no electrons are trapped in the bucket during the interaction,

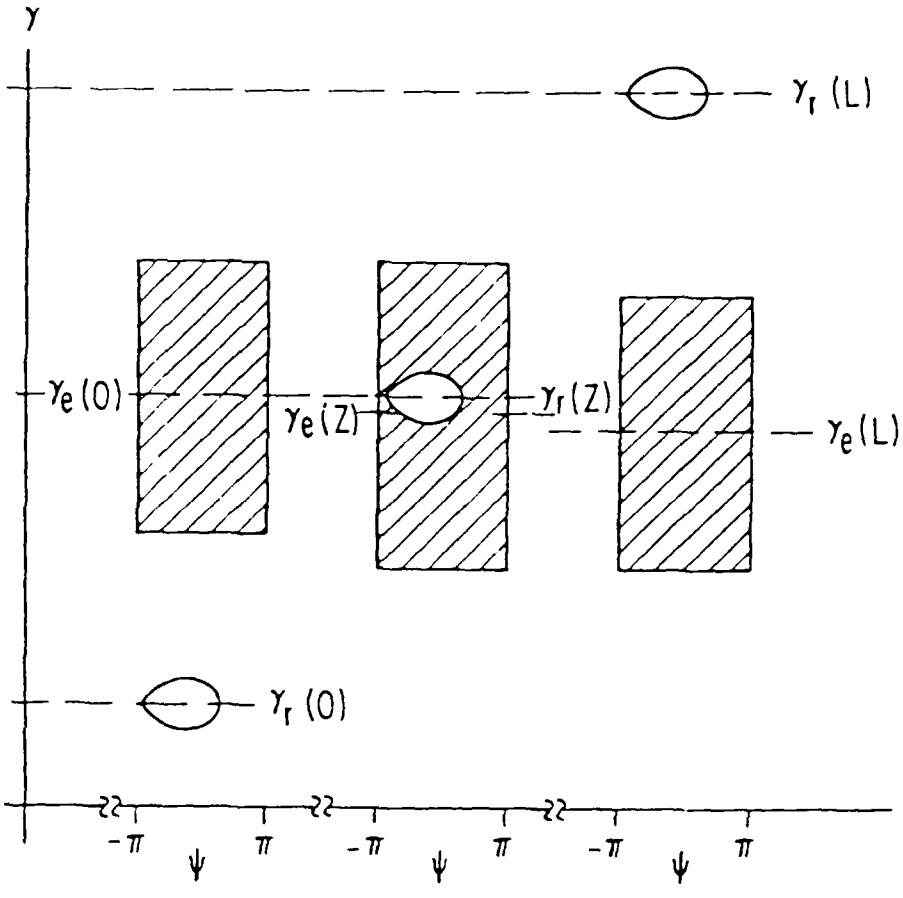

Figure 1. Motion of empty buckets through electron phase space in a phase area displacement FEL.

the final beam energy spread is nearly equal to the initial beam energy spread.

This method of beam energy extraction has two features which are attractive with respect to operating a variable parameter Free Electron Laser (FEL) oscillator in conjunction with a storage ring: (1) The energy extracted is insensitive to the beam energy spread; (2) The ratio of the energy extracted to the increase in the root mean square energy spread can be made to be small.

In practice, the bucket acceleration is never completely adiabatic and some energy spread will occur. Furthermore, a nonadiabatic entry and exit from the wiggler will induce additional energy spreads. Thus, such a device may be operated in steady state only if the increase in the effective phase space area occupied by the beam, due to the energy spreading on each passage through the wiggler, can be balanced by a corresponding decrease due to incoherent synchrotron radiation in the storage ring, and the beam energy boosted to compensate for the losses in the wiggler and storage ring. A convenient measure of efficiency is the ratio of the energy radiated in the wiggler to that lost in the storage ring during steady state operation. It is clearly desirable to maximize this ratio.

In this respect, we discuss an investigation of the efficiency of phase area displacement wigglers operated in a storage ring. The startup problem is first addressed in

Section I. The linear gain is calculated from an eigenmode analysis of the linearized FEL equations. This is followed in Section II by a comparison with numerical simulations of the theoretical estimates of beam energy loss and beam energy spread due to interaction of electrons with a finite amplitude ponderomotive potential well. In Section III, the results of numerical simulations of steady state operation is described, the efficiency is determined, and the scaling of efficiency with the wiggler and EM pulse parameters is derived.

A full self-consistent simulation would be very difficult to run since a very long EM pulse is required for adiabaticity, involving a correspondingly long electron micropulse and many particles. Our results must thus be interpreted only as necessary conditions in the design of phase area displacement wigglers.

II. LINEAR EIGENMODE ANALYSIS

In this section we address the small signal problem; i. e., growing the laser pulse from a very small amplitude.

It is assumed that the electron beam is relativistic with energy parameter $\gamma >> 1$ and that the beam self-fields are negligibly small (Compton regime). The periodic magnetic field wiggler (with wave number k_w and length L) and the EM pulse (with frequency ω_s and wave number k_s) are represented by circularly polarized vector potentials A_w and A_s with negligible spatial variations transverse to the direction of electron beam propagation. The EM pulse is approximated by a plane wave $A_s \exp(-i\omega_s t + ik_s z + i\zeta)$ with slowly varying amplitude A_s and phase ζ.

The electron equations of motion (in the resonant approximation) in terms of the electron energy and phase angle $(\hat{\gamma}, \psi)$ and the equations of the EM pulse amplitude A_s and phase ζ (from Maxwell's equations) are:

$$\frac{\partial \psi}{\partial v} = \hat{\gamma} \tag{1}$$

$$\frac{\partial \hat{\gamma}}{\partial v} = \Gamma + \frac{1}{2}\left[i\hat{a}e^{i\psi} - i\hat{a}^* e^{-i\psi}\right] \tag{2}$$

$$\frac{\partial \hat{a}}{\partial u} = i\eta h(u) \left\langle\!\left\langle e^{-i\psi} \right\rangle\!\right\rangle \tag{3}$$

where

$$u = \frac{c}{L}\left(\frac{z}{V} - t\right) \Big/ \left(\frac{c}{V} - 1\right)$$

$$v = \frac{c}{L}\left(t - \frac{z}{c}\right) \Big/ \left(\frac{c}{V} - 1\right)$$

$$\hat{\gamma} = \frac{2k_w L}{\gamma_r}\left(\gamma - \gamma_r\right) << 2k_w L$$

$$\psi = k_w z + k_s z - \omega_s t$$

$$\gamma_r = \left(\frac{k_s}{2k_w}\right)^{1/2}\left(1 + a_w^2\right)^{1/2}$$

$$\hat{a} = a e^{i\zeta} \equiv \frac{2k_w k_s L^2}{\gamma_r^2}\, a_w a_s\, e^{i\zeta}$$

$$\Gamma = \frac{2k_w L}{\gamma_r}\,\Delta\gamma_r$$

$$a_w = \frac{eA_w}{mc^2}$$

$$a_s = \frac{eA_s}{mc^2}$$

$$\frac{\eta}{u_o} = \frac{8(k_w L)^2}{\gamma_r(1 + a_w^2)}\,\frac{e\bar{I}}{mc^3}\left(\frac{L}{k_s r_o^2}\right) a_w^2 f$$

$$u_{\ell} = \frac{\ell k_s}{k_w L}$$

$$h(u) = \frac{L\left(1 - \frac{V}{c}\right)}{\ell} \frac{I(z,t)}{\bar{I}}$$

$$\int h(u)\,du = 1$$

$$\bar{I} = \frac{1}{\ell} \int I\,dz$$

V is the electron longitudinal velocity. a_w and k_w, and hence γ_r, are considered to be constant down the wiggler. The actual variable parameter wiggler is modeled by the inclusion of a constant electric field, that is $\dot{\gamma} \neq 0$. $\Delta\gamma_r$ is the change in γ which would be experienced by an electron freely accelerated by the electric field. ℓ is the nominal electron micropulse beam length. h(u) is a form factor determined by the beam profile. γ_0 is the beam radius and I is the beam current. f is the filling factor. The angular brackets imply integration over the initial energy distribution ($\hat{\gamma}_0$) and average over the initial phase (ψ_0) of the electrons:

$$\left\langle\left\langle e^{-i\psi} \right\rangle\right\rangle = \frac{1}{2\pi} \int_0^{2\pi} d\psi_0 \int d\hat{\gamma}_0\, F(\hat{\gamma}_0)\, e^{-i\psi}$$

$F(\hat{\gamma}_o)$ is the initial electron distribution function normalized so that $\int d\hat{\gamma}_o F(\hat{\gamma}_o) = 1$.

In the (u,v)-space, the wiggler ($L \geq z \geq 0$) lies between the lines $u + v = 0$ and $u + v = 1$. The electrons move on lines of constant u and the photons of the EM pulse, propagating in the beam direction, move on lines of constant v. The beam electrons and photons interact only when their trajectories in the (u,v)-plane intersect within the lines $u + v = 0$ and $u + v = 1$.

The electron phase space $(\hat{\gamma},\psi)$ trajectories are determined by the solutions of Equations (1) and (2), with initial conditions $\hat{\gamma} = \hat{\gamma}_o$, $\psi = \psi_o$ at $v = -u$. The phase of the electrons entering the wiggler is uncorrelated with that of the EM pulse. Thus, ψ_o is distributed uniformly between 0 and 2π.

To model a phase area displacement wiggler, a constant decelerating electric field ($\Gamma < 0$) is applied to decelerate the electrons. At the front of the wiggler, the electron energy is greater than the resonant energy, $\hat{\gamma}(0) = \hat{\gamma}_i > 0$. As the electrons move down the wiggler, $\hat{\gamma}$ decreases, passes through zero (at which point the electrons are in resonance with the ponderomotive potential well), and is negative at the back of the wiggler (the beam energy is less than the resonant energy, $\hat{\gamma}(L) = \hat{\gamma}_f < 0$). Thus, the deceleration of the electrons is used to model the increase of the resonant energy of the ponderomotive potential well from a value below

the beam energy at the front of the wiggler to a value above the beam energy at the back of the wiggler.

A determination of the linear gain from an eigenmode analysis of the linearized FEL equations has previously been discussed in the 1982 Annual Report for FEL oscillators with constant ($\Gamma = 0$) and variable parameter wigglers with $\Gamma > 0$. By following the same procedure, the linear gain for FEL oscillators with a phase area displacement wiggler ($\Gamma < 0$) can readily be derived.

In order to exploit the special properties of a phase area displacement wiggler, it is desirable to have an EM pulse with frequency such that the electrons (with mean energy $\hat{\gamma}$) are in resonance (with the ponderomotive potential well) near the middle of the wiggler, and with amplitude constant over many slippage distances so that the electron interaction is adiabatic. In order to grow an EM pulse with these characteristics, it will be necessary to provide for frequency discrimination (by passing the pulse through a narrow band pass filter) to select the mode with the desired frequency, and to use long electron micropulses. Thus, it is relevant to restrict the analysis of linear gain to long, constant amplitude EM pulses and correspondingly long electron micropulses. In this limit, the emerging EM pulse is $a(L) = e^{\delta}a(0)$, where the linear gain and phase shift per pass δ ($|\delta| < 1$) is easily derived from Equations (1) through (3) to be:

$$\delta = \frac{i\eta_o}{2} \int d\hat{\gamma}_o \, F(\hat{\gamma}_o) \int_o^1 dz \int_o^z dz' \, (z - z')$$

$$\exp\left\{ i\hat{\gamma}_o (z' - z) + \frac{i\Gamma z'^2}{2} - \frac{i\Gamma z^2}{2} \right\} \qquad (4)$$

If the mirror losses are included, the gain per pass is $1 - r + \delta$. $(1 - r)$ is the fractional reduction in amplitude per pass due to energy losses at the mirrors, and $\eta_o = \eta/u_o$.

If we take $F(\hat{\gamma}_o)$ to be Lorentzian

$$F(\hat{\gamma}_o) = \frac{1}{\pi \bar{\gamma}_{th}} \frac{1}{\left[1 + (\hat{\gamma}_o - \bar{\gamma})^2 / \bar{\gamma}_{th}^2\right]}$$

where $\bar{\gamma}$ is the mean energy and $\bar{\gamma}_{th}$ the energy spread, we obtain for $\Gamma = -|\Gamma|$, $|\Gamma|^{\frac{1}{2}} >> 1$,

$$1 - r + \delta = \frac{\eta_o}{4|\Gamma|^{3/2}} \left[(i - 1) \, Z\left(\frac{(i - 1)\varepsilon}{2}\right) - (i + 1) \, Z\left(\frac{(1 - i)(i\varepsilon + |\Gamma|^{\frac{1}{2}})}{2}\right) \right] \qquad (5)$$

where $$\varepsilon = \frac{\bar{\gamma}_{th} + i\bar{\gamma}}{|\Gamma|^{\frac{1}{2}}}$$

and $$Z(\sigma) = 2i e^{-\sigma^2} \int_{-\infty}^{i\sigma} d\xi \, e^{-\xi^2} .$$

Since $\bar{\gamma} \approx \frac{|\Gamma|}{2}$ implies $|\varepsilon| >> 1$, the function $Z(\mathcal{O})$ may be approximated by its asymptotic expansion:

$$Z(\mathcal{O}) = 2i\pi^{\frac{1}{2}} \exp(-\mathcal{O}^2) - \frac{1}{\mathcal{O}}(1 + 1/2\mathcal{O} + \ldots), \quad \mathrm{Im}\,\mathcal{O} < 0 \quad .$$

Thus, if $\bar{\gamma}_{th} = 0$,

$$1 - r + \delta = \frac{\eta_o \pi^{\frac{1}{2}}}{2|\Gamma|^{\frac{3}{2}}} \left[-(1+i) \exp\left(\frac{-i\bar{\gamma}^2}{2|\Gamma|}\right) + (1-i) \exp\left(\frac{i(|\Gamma| - \bar{\gamma})^2}{2|\Gamma|}\right) \right] \quad . \tag{6}$$

The linear gain oscillates as $\bar{\gamma}$ varies and will be significantly modified by a finite energy spread.

If the energy spread is finite with

$$\pi^{\frac{1}{2}} \exp\left(\frac{-\bar{\gamma}_{th}\bar{\gamma}}{|\Gamma|}\right) << \frac{1}{|\varepsilon|}$$

and

$$\pi^{\frac{1}{2}} \exp\left\{-\bar{\gamma}_{th}(1 - \bar{\gamma}/|\Gamma|)\right\} << \frac{1}{|\varepsilon - i|\Gamma|^{\frac{1}{2}}|}$$

$$1 - r + \delta = \frac{i\eta_o}{2|\Gamma|\ \varepsilon(\varepsilon - i|\Gamma|^{\frac{1}{2}})}$$

and

$$\text{Re}\ (1 - r + \delta) = \frac{\eta_o \bar{\gamma}_{th} \left(2\bar{\gamma} - |\Gamma|\right)}{2\left(\bar{\gamma}_{th}^2 + \bar{\gamma}^2\right)\left(\bar{\gamma}_{th}^2 + (\bar{\gamma} - \Gamma)^2\right)}$$

$$\approx \frac{8\eta_o \bar{\gamma}_{th}}{|\Gamma|^3} \left(2\bar{\gamma}/|\Gamma| - 1\right), \ \bar{\gamma}_{th} < \bar{\gamma} \approx |\Gamma|/2 \quad . \tag{7}$$

The linear gain is reduced in magnitude and is positive only when $\bar{\gamma} > |\Gamma|/2$. As will be apparent subsequently when model parameters are discussed, the energy spreads to be expected are such that Equation (7) is applicable and the predicted linear gain is too small to be useful. Thus, an alternate startup strategy is required; e.g.,

(a) Using another laser for startup.

(b) Varying electron energy so that electrons are initially resonant at wiggler entrance or exit. This is a complex scenario and it is not clear that it is feasible when the transition phase is considered.

In the remainder of this report, we assume that this problem has somehow been solved and that a long laser pulse of large constant amplitude is available.

III. BEAM ENERGY LOSS AND ENERGY SPREAD

The electron equations of motion [Equation (1) and Equation (2)] are derivable from the Hamiltonian $\bar{H}(\hat{\gamma},\psi)$:

$$\bar{H}(\hat{\gamma},\psi) = \frac{\hat{\gamma}^2}{2} - \Gamma\psi - a\cos(\psi + \zeta)$$

$$\equiv \frac{\hat{\gamma}^2}{2} + V(\psi) \qquad (8)$$

Analytic estimates of the beam energy loss and beam energy spread can be obtained in the limit where a and ζ are constant.

In this limit, $\bar{H}$ is a constant of the motion. The electrons see a potential well $V(\psi) = -\Gamma\psi - a\cos\psi$ (set $\zeta = 0$), which is plotted in Figure 2 for $\Gamma < 0$. The stationary points of $V(\psi)$ occur at

$$\psi = 2N\pi + \psi_r,\ 2N\pi + \pi\,\mathrm{sign}(\psi_r) - \psi_r$$

where

$$\sin\psi_r = \Gamma/a$$

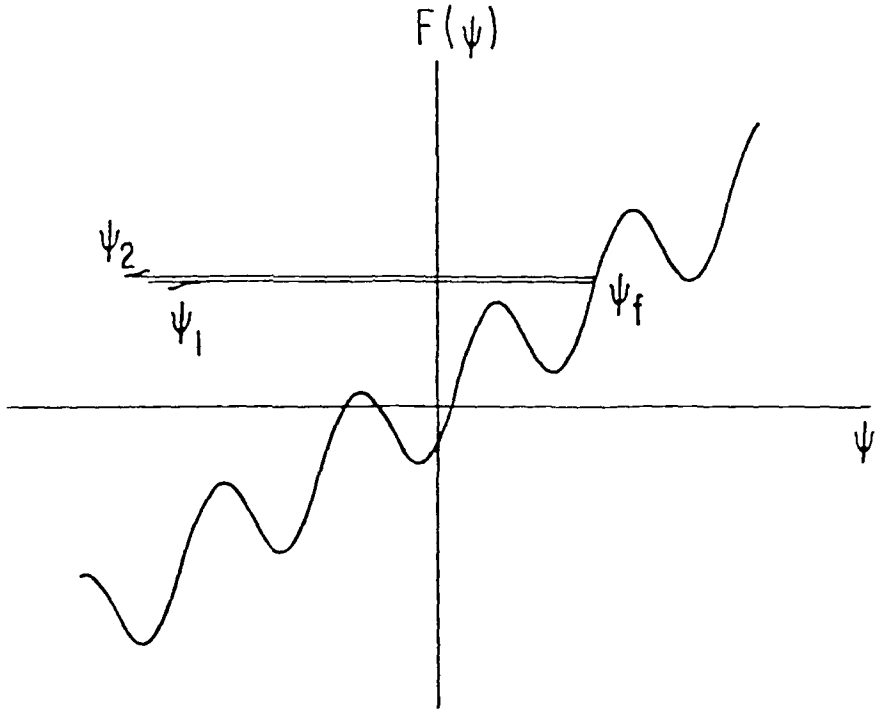

Figure 2. Electron phase trajectory in the ponderomotive potential of a phase area displacement wiggler.

the potential well depth is:

$$\Delta V = 2a \left\{ \cos \psi_r + \sin \psi_r \left(\psi_r - \frac{\pi}{2} \text{ sign } (\psi_r) \right) \right\}$$

corresponding to a bucket height $\delta\hat{\gamma}_{max}$ of

$$\delta\hat{\gamma}_{max} = 2a^{\frac{1}{2}} \left[\cos \psi_r + \sin \psi_r \left(\psi_r - \frac{\pi}{2} \text{ sign } (\psi_r) \right) \right]^{\frac{1}{2}}$$

The difference in adjacent maxima is

$$\Delta\hat{\gamma}_{max} = 2\pi |\Gamma|$$

$$= 2\pi a \sin |\psi_r| \quad .$$

A typical trajectory in the ponderomotive potential well is shown in Figure 2. The electron phase ψ increases from an initial value ψ_1, reaches a maximum ψ_f when it is "reflected," and then decreases to a final value ψ_2. Note that if the amplitude a is increasing, the electrons may become trapped. Thus the wiggler should be designed to provide a very slow decrease in bucket height. Note also that the amplitude cannot be allowed to fluctuate in time, thus requiring a very strong optical filter.

Thus, by integrating Equations (1) and (2) through the wiggler, the net change in the electron energy due to interaction with the ponderomotive potential well is:

$$\Delta\hat{\gamma} = \left[\hat{\gamma} - \Gamma v\right]_{v=0}^{v=1}$$

$$= -\int_{\psi_1}^{\psi_F} \frac{a \sin\psi \, d\psi}{\sqrt{2(\bar{H} - V(\psi))}} + \int_{\psi_F}^{\psi_2} \frac{a \sin\psi \, d\psi}{\sqrt{2(\bar{H} - V(\psi))}}$$

$$\approx -\sqrt{2}\,\hat{a}_s \sin\psi_r$$

$$\int_{-\infty}^{\psi_F} d\psi \left[\frac{1}{\sqrt{\bar{H} + a(\psi \sin\psi_r + \cos\psi)}} \right.$$

$$\left. - \frac{1}{\sqrt{\bar{H} + a(\psi \sin\psi_r + \cos\psi_F)}} \right] \qquad (9)$$

where γ_F is determined by $\bar{H} = -\Gamma\psi_F - a\cos\psi_F$.

The integrals in Equation (9) have been evaluated in Reference 1 and the following estimates obtained of the beam energy loss and root mean square energy spread:

$$\Delta\bar{\hat{\gamma}} = -\frac{8}{\pi}(a)^{1/2} \equiv -\Delta\bar{\gamma}_L \qquad (10)$$

$$\left(\Delta\hat{\gamma}_{rms}\right)_{wiggler} = |\sin\psi_r|\Delta\bar{\gamma}_L \quad . \qquad (11)$$

A further energy spread can occur if the beam entry into and beam exit out of the wiggler is nonadiabatic. This contribution to the room mean square energy spread is estimated to be

$$\left(\Delta\hat{\gamma}_{rms}\right)_{ends} \approx \frac{2a}{\Gamma} \tag{12}$$

where the mean initial energy $\bar{\gamma} \sim \Gamma/2$. However, the magnitude of this contribution can be essentially eliminated by a gradual tapering of the front and back of the wiggler so that the beam enters and exits the wiggler adiabatically.

If the end contributions are taken to be statistically independent of the wiggler contributions, the total root mean square energy spread is:

$$\frac{\Delta\hat{\gamma}_{rms}}{\Delta\bar{\gamma}_L} \approx \sqrt{\frac{\Gamma^2}{a^2} + \frac{\pi^2 a}{16\Gamma^2}} \tag{13}$$

The theoretical estimates of $\Delta\bar{\gamma}_L$ and $\Delta\hat{\gamma}_{rms}$, Equations (10) and (13), have been compared with the results of numerical simulation of a one-dimensional FEL with a phase area displacement wiggler.

In the simulations, a monoenergetic electron beam with energy $\hat{\gamma} = \hat{\gamma}_i$, distributed uniformly in phase angle, is injected into the wiggler. The transitions into and out of the wiggler were step-functions, and hence nonadiabatic. The

mean energy $\bar{\gamma}_f$ and energy spread $\Delta\gamma_{rms}$ on exit from the wiggler are evaluated. The results for one set of FEL parameters (610 particles are used in the simulations) are shown in Table 1.

It may be noted that when the initial beam energy $\hat{\gamma}_i$ is such that the electrons are in resonance with the ponderomotive potential well inside the wiggler ($\Gamma - 2a^{\frac{1}{2}} > \hat{\gamma}_i > 2a^{\frac{1}{2}}$), the simulation results are consistent with the theoretical picture of an average energy loss ($\Delta\bar{\gamma} \approx 204$) and an average energy spread ($\Delta\gamma_{rms} \approx 40.0$) independent of the initial energy, although the simulated loss was about 20 percent lower and the spread about 25 percent higher than predicted by the crude theory.

No significant trapping is observed except when the electrons are in resonance at the beginning or end of the wiggler. When trapping occurs at the beginning of the wiggler, the energy spread is considerably enhanced as the trapped electrons are dragged along in phase space by the ponderomotive potential well.

TABLE 1

$a = 10^4$ $\Gamma = -1000$

$\hat{Y}_i$	$\Delta\bar{Y} = \hat{Y}_i - \bar{Y}_f$	$\Delta\hat{Y}_{rms}$
150	-212	529
170	-58	436
200	212	62.1
250	214	35.7
300	207	49.9
350	198	34.7
400	197	34.6
450	202	42.4
500	207	30.7
550	205	44.2
600	203	38.1
650	203	40.0
700	212	32.8
750	191	39.1
800	203	32.6
850	204	40.3
900	203	42.1
950	199	58.7
1000	196	63.4

IV. STORAGE RING OPERATION

An FEL oscillator with a phase area displacement wiggler can be operated in steady state with a storage ring if the increase in energy spread can be balanced by a decrease due to incoherent synchrotron radiation and the beam energy boosted by a radio-frequency (RF) cavity to compensate for the losses in the wiggler and in synchrotron radiation.

The energy loss $\Delta\gamma_{syn}$ due to synchrotron radiation is proportional to γ^2, $\Delta\gamma_{syn} = -S_o\gamma^2$. In terms of the dimensionless variable $\hat{\gamma}$:

$$\begin{aligned}
\Delta\hat{\gamma}_{syn} &= -S_o \frac{2k_wL}{\gamma_r}\,\gamma_r^2 \left(1 + \frac{\hat{\gamma}}{2k_wL}\right)^2 \\
&= -S_o \frac{2k_wL}{\gamma_r}\,\gamma_r^2 \left(1 + \frac{\bar{\gamma}}{2k_wL}\right)^2 \left\{1 + \frac{\hat{\gamma} - \bar{\gamma}}{k_wL(1 + \bar{\gamma}/2k_wL)} \cdots\right\} \\
&\equiv -\Delta\bar{\gamma}_{syn} \left\{1 + \frac{\hat{\gamma} - \bar{\gamma}}{k_wL} + \cdots\right\}
\end{aligned} \tag{14}$$

The energy change per pass $\Delta\hat{\gamma}$ is the sum of three terms:

$$\Delta\hat{\gamma} = \Delta\hat{\gamma}_{syn} + \Delta\bar{\gamma}_{RF} - \Delta\bar{\gamma}_{L}$$

$$= -\Delta\bar{\gamma}_{syn}\left\{1 + \frac{\hat{\gamma} - \bar{\gamma}}{k_w L}\right\} + \Delta\bar{\gamma}_{RF} - \Delta\bar{\gamma}_{L} \qquad (15)$$

where $\Delta\bar{\gamma}_{RF}$ is the energy increase in the RF cavity. To attain steady state operation, $\Delta\bar{\gamma}_{RF}$ is required to compensate for the total mean energy losses, $\Delta\bar{\gamma}_{syn} + \Delta\bar{\gamma}_{L}$.

The presence of a storage ring can therefore be included in the simulations previously described by recirculating the electrons through the wiggler while modeling the effect of the storage ring on the electron energy with the following equation:

$$\hat{\gamma}_i^{(n+1)} = \sigma\,\hat{\gamma}_f^{(n)} + b \qquad (16)$$

where $\hat{\gamma}_f^{(n)}$ is the value of $\hat{\gamma}$ on exit from the wiggler on the n^{th} pass, and $\hat{\gamma}_i^{(n+1)}$ the input value of $\hat{\gamma}$ on the $(n+1)^{th}$ pass. The parameter σ is related to $\Delta\bar{\gamma}_{syn}$ by

$$\sigma = 1 - \frac{\Delta\bar{\gamma}_{syn}}{k_w L} \quad . \qquad (17)$$

The parameter b is determined by the requirement that the mean input energy of the beam on each pass is maintained constant.

The simulations are carried out for a given wiggler design with the value of σ (and hence the synchrotron energy loss $\Delta\bar{\gamma}_{syn}$) adjusted until an efficient steady state operation is obtained. This is achieved when $\Delta\bar{\gamma}_{syn}$ is just large enough to limit the energy spread so that electron trapping is negligible. Electron trapping is undesirable, particularly when it occurs at the beginning of the wiggler, since it results in considerably enhanced energy spreading.

The evolution of the electron distribution function F per pass may be described by a Fokker Planck equation, and in steady state

$$\frac{1}{2} \frac{\partial^2}{\partial \hat{\gamma}^2} \langle (\Delta\hat{\gamma})^2 \rangle F - \frac{\partial}{\partial \hat{\gamma}} \langle \Delta\hat{\gamma} \rangle F = 0 \qquad (18)$$

where the energy spread in the wiggler

$$\left\langle (\Delta\hat{\gamma})^2 \right\rangle = \left(\Delta\hat{\gamma}_{rms}\right)^2$$

is balanced by the synchrotron damping in the storage ring

$$\langle \Delta\hat{\gamma} \rangle = - \Delta\bar{\gamma}_{syn} \frac{(\hat{\gamma} - \bar{\gamma})}{k_w L}$$

If the dependence of $\left(\Delta\hat{\gamma}_{rms}\right)^2$ on $\hat{\gamma}$ is neglected, the solution of Equation (18) is:

$$F = C_o \exp\left[- \frac{\Delta\bar{\gamma}_{syn}}{k_w L} \frac{(\hat{\gamma} - \bar{\gamma})^2}{(\Delta\hat{\gamma}_{rms})^2} \right] \tag{19}$$

where C_o is a normalization constant.

An approximate theoretical criterion for negligible trapping in steady state may therefore be obtained by restricting the fraction of electrons which can be in resonance with the ponderomotive potential well at the beginning of the wiggler to less than 10^{-5}. This imposes the following lower limit on $\Delta\bar{\gamma}_{syn}$:

$$\frac{\Delta\bar{\gamma}_{syn}}{k_w L} > \left|\log 10^{-4}\right| \frac{(\Delta\hat{\gamma}_{rms})^2}{(\bar{\gamma} - 2a^{\frac{1}{2}})^2} \tag{20}$$

where $\bar{\gamma} \sim |\Gamma|/2$ so that electrons with the mean beam energy are in resonance near the center of the wiggler.

The accuracy of this criterion has been estimated by comparison with numerical simulations for a wiggler design with the following physical parameters.

B_w	8 kG
γ_r	10^3
k_s	$2\pi \times 10^4$ cm^{-1}
L	2×10^4 cm
$k_w L$	1.77×10^4
Peak Circulating Power	4.9 GW/cm^2
Change in Resonant Energy	$\Delta\gamma_r = 28$

The corresponding simulation parameters are:

$$a = 10^4$$
$$|\Gamma| = 10^3$$

and $\bar{\gamma}$ was set equal to

$$\bar{\gamma} = |\Gamma|/2.$$

The observed minimum value of $\Delta\bar{\gamma}_{syn}/k_wL$ for which no significant electron trapping occurred after 200 steady state passes (using 123 particles for each pass) is

$$\frac{\Delta\bar{\gamma}_{syn}}{k_wL} \approx 0.075 \quad . \tag{21}$$

The observed energy loss in the wiggler is

$$\Delta\bar{\gamma}_{laser} \approx 205 \tag{22}$$

and hence

$$\left(\frac{\Delta\bar{\gamma}_{laser}}{\Delta\bar{\gamma}_{syn}}\right)_{simulation} \approx 0.15 \quad . \tag{23}$$

This ratio is a measure of the FEL steady state efficiency.

The theoretical estimate of $\Delta\bar{\gamma}_{syn}/k_wL$ obtained from Equation (20) with $\Delta\hat{\gamma}_{rms}$ determined by Equation (13) and $\Delta\bar{\gamma}_L$ by Equation (10) is

$$\frac{\Delta\bar{\gamma}_{syn}}{k_w L} \sim 0.11 \quad . \tag{24}$$

It is larger than the observed value [Equation (21)] by a factor of 1.4. The difference may be attributed to the dependence of $\Delta\hat{\gamma}_{rms}$ on $\hat{\gamma}_i$. Since $\Delta\bar{\gamma}_{laser} = \Delta\bar{\gamma}_L$ is somewhat larger than the observed value [Equation (22)], the theoretical estimate of FEL efficiency

$$\left(\frac{\Delta\bar{\gamma}_{laser}}{\Delta\bar{\gamma}_{syn}}\right)_{theory} \approx 0.13$$

is close to that seen in the simulations.

The scaling of efficiency with wiggler and EM pulse parameters may be obtained from Equation (20) by substituting Equation (11) for $\Delta\hat{\gamma}_{rms}$ (the energy spreading due to nonadiabatic entry and exit is assumed negligible):

$$\frac{\Delta\bar{\gamma}_{laser}}{\Delta\bar{\gamma}_{syn}} \lesssim \frac{\pi}{295} \frac{a^{3/2}}{k_w L} \left(1 - \frac{4a^{1/2}}{|\Gamma|}\right)^2$$

$$= \frac{8\pi}{295} k_w^2 L^2 \left(\frac{a_w a_s}{1 + a_w^2}\right)^{3/2} \left(1 - \frac{4a^{1/2}}{|\Gamma|}\right)^2 \tag{25}$$

where $\bar{\gamma} = |\Gamma|/2$ and $a > |\Gamma| > 4a^{1/2}$.

As can be seen from the preceding discussion of the comparison between theory and simulation, the numerical coefficient is perhaps uncertain by about 50 percent.

V. DISCUSSION

In order to obtain good efficiency during steady state operation, it is essential that the electron interaction with the ponderomotive potential well be adiabatic and that electron trapping be negligible.

Furthermore, a long constant amplitude EM pulse is necessary to produce a potential well which remains unchanged through the wiggler. Variations of the potential well can affect not only adiabaticity, but lead to electron trapping. As a general rule, the electrons should "see" negligible amplitude fluctuations in a traversal time across a "bucket." The slippage ΔZ of the electrons in the EM pulse during traversal through the "bucket" in which reflection occurs (Figure 2) is estimated to be

$$\Delta Z \sim L\left(\frac{c}{v}-1\right)\frac{\pi}{\sqrt{2a}}\ \ell n\ \frac{\pi a}{4|\Gamma|}\ ,\quad \frac{a}{|\Gamma|} >> 1$$

excluding those exponentially few electrons "caught" at the top of the potential well. Thus, an approximate criterion for restricting the probability of trapping to less than τ (due to increases Δa in amplitude) is obtained by demanding

$$\frac{da}{dz}\ \Delta z \sim \Delta a < \tau a$$

that is

$$\frac{1}{a}\frac{da}{dz} < \frac{\tau/(2a)^{1/2}}{L\left(\frac{c}{v}-1\right)\pi \ell n\left(\frac{\Gamma a}{4|\Gamma|}\right)} \qquad (26)$$

The fraction τ of electrons which are trapped are presumably accelerated to high energies and must be replaced or reprocessed.

For $a = 10^4$ and $\Gamma/a = 10^{-1}$ and $\tau = 10^{-4}$,

$$\frac{1}{a}\frac{da}{dz} < \frac{1}{460L\left(\frac{c}{v}-1\right)}$$

which implies slow amplitude variations over many slippage distances.

For the numerical example discussed earlier, this implies pulse lengths of 5 cm.

When the above conditions are satisfied, the FEL efficiency in steady state is estimated to be [Equation (25)]:

$$\frac{\Delta\bar{\gamma}_{laser}}{\Delta\bar{\gamma}_{syn}} \lesssim 0.048\, k_w^2 L^2 \left(\frac{a_w}{1+a_w^2}\right)^{3/2} \left(\frac{P(GW)}{k_s^2 r_p^2}\right)^{3/4} \left(1-\frac{4a^{1/2}}{|\Gamma|}\right)^2 \qquad (27)$$

where the dimensionless pulse amplitude $|a_s|$ is related to the power P(GW) in gigawatts of the EM pulse (assumed to be circularly polarized) by

$$P(GW) = 0.69\pi \; k_s^2 r_p^2 \left|a_s\right|^2$$

πr_p^2 is the effective area of the pulse.

If the wiggler length L is taken to be the Rayleigh diffraction length $L_R = k_s r_p^2$, Equation (27) reduces to

$$\frac{\Delta\bar{\gamma}_{laser}}{\Delta\bar{\gamma}_{syn}} < 0.029 \frac{\left(k_w L_R\right)^{5/4}}{\gamma_r^{3/2}} \; P^{3/4} \left(\frac{a_w^2}{1 + a_w^2}\right)^{3/4} \left(1 - \frac{4a^{1/2}}{|\Gamma|}\right)^2 \qquad (28)$$

The extracted beam energy $\Delta\hat{\mathcal{E}}(ev)$ in electron volts per pass is

$$\Delta\hat{\mathcal{E}}(ev) = 0.511 \times 10^6 \; \gamma_r \frac{\Delta\hat{\gamma}_{laser}}{2k_w L}$$

and the power $\Delta P(GW)$ transferred per pass to the EM pulse from the electron micropulse with peak current I(amps) in amperes is

$$\Delta P(GW) = 5.11 \times 10^{-4} \; \gamma_r \frac{4a^{1/2}}{\pi k_w L} \; I(amps)$$

$$= 1.43 \times 10^{-3} \; \gamma_r \left(\frac{a_w}{1 + a_w^2}\right)^{1/2} \left(\frac{P(GW)}{\pi k_s^2 r_p^2}\right)^{1/4} I(amps) \qquad (29)$$

In steady state, the power lost by the EM pulse at the mirrors equals the power gained from the electron micropulse:

$$\Delta P(GW) = 2(1 - r)\, P(GW) \tag{30}$$

and hence the current required to maintain steady state for a given value of the fractional power loss $2(1 - r)$ is:

$$I(\text{amps}) = 1.40 \times 10^3 \frac{(1 - r)}{\gamma_r} \left(\frac{1 + a_w^2}{a_w}\right)^{\frac{1}{2}} \left(\pi k_s^2 r_p^2\right)^{\frac{1}{4}} P^{3/4}(GW)$$

$$= 1.4 \times 10^3 \frac{(1 - r)}{\gamma_r^{\frac{1}{2}}} \left(2\pi k_w L_R\right)^{\frac{1}{4}} \left(\frac{1 + a_w^2}{a_w^2}\right)^{\frac{1}{4}} P^{3/4}(GW) \ ,$$

$$L = L_R = k_s r_p^2 \tag{31}$$

In the case of the physical parameters described in Section IV where the peak circulating power is $P = 4.9$ GW, $k_s = 2\pi \times 10^4$ cm^{-1}, $\gamma_r = 10^3$, $a_w = 5.3$, if the power loss is 1%, $2(1 - r) = 0.01$ and $\pi r_p^2 = 1$ cm , the peak electron micropulse current is $I = 13.5$ amperes.

This limit on the peak micropulse current is not particularly severe.

A more severe constraint arises if the operation of the FEL oscillator is to be initiated by growing the desired EM pulse from noise levels. The peak current density must then

be large enough to produce adequate linear gain per pass to overcome the energy losses at the mirrors. For long electron micropulses with finite energy spreads, the linear gain per pass for a long constant amplitude EM pulse is determined by Equation (7):

$$\mathrm{Re}\,\delta \approx 3.76 \times 10^{-3} \frac{k_w^2 L^3}{\gamma_r k_s r_o^2} \frac{a_w^2 f}{\left(1 + a_w^2\right)} I(\text{amps}) \cdot \frac{\bar{\gamma}_{th}}{|\Gamma|^3} \left(\frac{2\bar{\gamma}}{|\Gamma|} - 1\right) \quad . \tag{32}$$

If the energy spread is taken to be [Equation (20)], the maximum allowable,

$$\bar{\gamma}_{th}^2 = \frac{\left(\Delta\hat{\gamma}_{rms}\right)^2 k_w L}{2\Delta\hat{\gamma}_{syn}} \approx \frac{\left(\frac{|\Gamma|}{2} - 2a^{\frac{1}{2}}\right)^2}{18.4} \quad ,$$

the linear gain for the example previously described, where $I = 13.5$ amps and the beam area is taken to be $\pi r_o^2 = 1\ \mathrm{cm}^2$, is

$$\mathrm{Re}\,\delta = 1.1 \times 10^{-3} \left(\frac{2\bar{\gamma}}{|\Gamma|} - 1\right) f \quad .$$

This value of the linear gain is somewhat on the low side to overcome any reasonable mirror losses. Higher micropulse peak currents or alternative startup strategies would probably be required.

Even if the wiggler and beam parameters can be designed so that finite linear gain is obtained, there remains the

issue of accessibility to the desired final steady state operation. Further investigations are needed to determine the evolution of the EM pulse from noise levels.

In summary, high FEL efficiency is theoretically possible for FEL oscillators using a phase area displacement wiggler in conjunction with a storage ring. Long wigglers containing many wiggler periods and EM pulses with large circulating peak powers are effective in obtaining high efficiencies. Very smooth long pulses are required to avoid trapping, hence good frequency discrimination. The linear gain per pass tends to be small unless appreciable micropulse peak current densities are available. The scenario of the time evolution to a steady state is complex and remains to be elucidated.

REFERENCE

1. N. M. Kroll, P. Morton and M. N. Rosenbluth, "Free Electron Lasers with Variable Parameter Wigglers," IEEE Journal of Quantum Electronics, Vol. QE-17, pp. 1436-1468 (1981).

A P P E N D I X E

TWO-DIMENSIONAL EFFECTS IN FREE ELECTRON LASERS

I. INTRODUCTION

The motion of electrons in a free electron laser under the combined influence of the wiggler magnets and electromagnetic wave may be calculated from the particle Hamiltonian as discussed below. This problem has hitherto been considered essentially as a one-dimensional problem in which the electron's motion can be reduced to the pendulum equation in the "ponderomotive" potential formed by the wiggler and laser magnetic fields.[1] In particular, high efficiency "tapered wiggler" configurations rely on electrons being trapped and executing "synchrotron" oscillations in this potential.

It is the purpose of this note to extend that description by taking account of the fact that the fields actually depend on transverse dimensions. To simplify our discussion, we will consider transverse dependence on only a single coordinate, x. The most obvious consequence of the transverse (focusing) variation of the wiggler magnetic field is that the electron undergoes transverse betatron

oscillations. In the simplest approximation, the betatron and synchrotron oscillations are decoupled, since one is transverse and the other longitudinal insofar as the laser pulse may be treated as a plane wave. Herein we propose to analyze the coupling which results from such physical effects as curvature of the optical wave front. Radial variation of optical amplitude introduces effects similar to but somewhat smaller than those we consider here.

II. DERIVATION OF DRIVEN PENDULUM EQUATION

It is conventional to express the vector potential in dimensionless units $a = eA/mc^2$. We denote by subscript w quantities relating to the wiggler magnet and by subscript s those relating to the laser field.

Hence the vector potential is $\vec{A} = A_y\hat{y}$ with

$$A_y = a_w \cosh k_w x \cos k_w z$$

$$- a_s (x,z,t) \cos [k_s(z - ct) - \phi(x,z,t)] . \quad (1)$$

Typically $a_w \sim \mathcal{O}(1)$ and $a_s \sim \mathcal{O}(10^{-3})$.

The transverse dependence of the laser amplitude and phase are presumed given. We will concentrate our attention on phase behavior near $x = 0$ where $\phi \sim k_s x^2/R$ with R the effective radius of curvature of the wave front. As a specific example, we sometimes consider a low gain oscillator for which the laser pulse in the optical cavity will be well described by a Gaussian mode

$$a_s \sim \left(x_\circ^2 + \frac{2i\,z}{k_s}\right)^{-\frac{1}{2}} \times \exp\left(-x^2/\left|x_\circ^2 + 2i\,z/k_s\right|\right)$$

with x_0 the width of the beam waist and z the distance from the optical waist. For such a pulse

$$\frac{1}{R} = \frac{1}{2Z_R} \frac{z/Z_R}{1+\left(z/Z_R\right)^2} \tag{2}$$

with the Rayleigh length $Z_R = k_s x_0^2/2$.

We may use the canonical momentum p_z as our Hamiltonian with (x, p_x, γ, t) as the canonical coordinates and z the independent variable.[2] Taking $\gamma >> 1$, $k_w x << 1$, $a_s << 1$, we find

$$p_z \equiv \gamma - \frac{1}{2\gamma} \left\{ 1 + p_x^2 + a_w^2 \left[1 + k_w^2 x^2\right] \cos^2 k_w z \right.$$
$$\left. - 2a_w a_s \cos k_w z \cos\left[k_s(z - ct) - \phi\right] \right\}$$

Averaging over the fast wiggler oscillations and keeping only the term in the cross product which allows for near electron resonance, we find for the averaged Hamiltonian

$$p_z \equiv \gamma - \frac{1}{2\gamma} \left\{ 1 + p_x^2 + \frac{a_w^2}{2} \left(1 + k_w^2 x^2\right) \right.$$
$$\left. - a_w a_s \cos\left[\left(k_w + k_s\right) z - k_s t - k_s \frac{x^2}{R}\right] \right\} \tag{3}$$

Recalling that $a_w << a_s$ we find for the transverse motion the decoupled betatron equation

$$\frac{d^2x}{dz^2} = -\frac{k_w^2 a_w^2}{2\gamma^2} x \equiv -k_\beta^2 x \qquad (4)$$

with solution $x = x_\beta \cos(k_\beta Z + \delta)$.

For the longitudinal motion we have

$$\frac{dt}{dz} = 1 + \frac{1 + \frac{a_w^2}{2} + p_x^2 + \frac{k_w^2 a_w^2 x^2}{2}}{2\gamma^2}$$

$$\equiv 1 + \frac{1 + \frac{a_w^2}{2}\left(1 + k_w^2 x_\beta^2\right)}{2\gamma^2} \qquad (5)$$

and

$$\frac{d\gamma}{dz} = -\frac{k_s a_w a_s}{2\gamma} \sin\left[\left(k_w + k_s\right) z - k_s t - k_s \frac{x^2}{R}\right] . \qquad (6)$$

It is convenient to rewrite Equation (5) in terms of the optical phase

$$\psi = \left(k_w + k_s\right) z - k_s ct - k_s \frac{x^2}{R} , \qquad (7)$$

$$\frac{d\psi}{dz} = k_w - \frac{k_s\left(1 + \frac{a_w^2}{2}\left(1 + k_w^2 x_\beta^2\right)\right)}{2\gamma^2}$$

$$+ \frac{k_s x_\beta^2}{R} k_\beta \sin(2k_\beta z + 2\delta) \quad . \qquad (8)$$

Combining Equations (6)and (8), we recover the familiar pendulum equation with a driving term

$$\frac{d^2\psi}{dz^2} = - \frac{k_s^2\left(1 + \frac{a_w^2}{2}\left(1 + k_w^2 x_\beta^2\right)\right)}{2\gamma^4} a_w a_s \sin$$

$$+ \frac{2k_s k_\beta^2 x_\beta^2}{R} \cos(2k_\beta z + 2\delta)$$

or on introducing

$$\Omega_s = \frac{k_s}{(2)^{\frac{1}{2}}\gamma^2}\left[1 + \frac{a_w^2}{2}(1 + k_w^2 x_\beta^2)\right]^{\frac{1}{2}} (a_w a_s)^{\frac{1}{2}};$$

$$z' = \Omega_s z \; ; \; \alpha = \frac{2k_\beta}{\Omega_s} \; ; \; \beta = \frac{1}{2}\frac{k_s x_\beta^2}{R}\alpha^2 \; ;$$

we have our fundamental equation

$$\frac{d^2\psi}{dz'^2} = -\sin\psi + \beta \sin(\alpha z' + 2\delta) . \qquad (9)$$

The phase δ may be chosen to be 0 without loss of generality.

Note that if x_β is comparable to the laser beam width x_o and if the wiggler length is of order a Rayleigh length, then $\beta \sim \mathcal{O}(\alpha^2)$. α depends on many parameters but typically $\alpha \gtrsim 1$, depending on whether the peak circulating power in the laser is less than or greater than 1 GW. These limits will be refined in the later discussion, but we anticipate by noting that the most interesting case will be the resonant case $\alpha \sim 1$, and that such a power level is likely to be realized during the buildup of a high power oscillator, or possibly in the operation of a high power amplifier.

III. BEHAVIOR OF THE BETATRON SYNCHROTRON RESONANCE

We now turn to solution of the basic differential Equation (9) treating α and β as given constants. The solution depends on whether α is greater, less than, or approximately equal to 1. We bear in mind that the primary interest is whether particles trapped near the bottom of the ponderomotive well become untrapped due to the driving term.

1. Case I - $\alpha << 1$, High Optical Power

In this case the driving term changes adiabatically and $\psi \approx \sin^{-1}\left|\beta \sin(\alpha z' + 2\delta)\right|$. Hence, the condition that particles remain trapped is simply $\beta < 1$, i.e., $\frac{1}{2}\frac{k_s x_\beta^2}{R}\alpha^2 < 1$. For a Gaussian pulse at the most unfavorable value $Z = Z_R$, we see from Equation (2) that this condition becomes $\frac{1}{4}\frac{x_\beta^2}{x_o^2}\alpha^2 < 1$. Since one must have $x_\beta \lesssim x_o$ in order that the electron remain in the optical field, it follows that no significant detrapping occurs in this regime.

2. Case II - $\alpha >> 1$, Low Optical Power

Here, since we are interested in particles with $\psi << 1$, an approximate solution is $\psi \sim \frac{\beta}{\alpha^2 - 1}\sin \alpha z'$, leading to an approximate condition for avoiding detrapping $3/\alpha^2 < \pi/2$ or for a Gaussian pulse $x_\beta^2/x_o^2 < 2\pi$ and again it would seem that this regime is not dangerous. The form of

the solution of course points out the potential dangers of the resonance region $\alpha \approx 1$.

3. Case III - $\alpha \simeq 1$

Insofar as α and β are constants, we may obtain an analytic approximate solution to Equation (9) as follows.

The Hamiltonian for Equation (9) is

$$H = \frac{\psi'^2}{2} - \cos\psi - \beta\psi \sin \alpha z'$$

If we introduce angle action variables[2] for the unperturbed ($\beta=0$) Hamiltonian, we have

$$H = \int \Omega dJ - \beta\psi(J,\phi) \sin \alpha z' \quad . \tag{10}$$

Here

$$J \equiv \int \psi' \, d\psi = \frac{8}{\pi} \left\{E(k^2) - (1 - k^2) \, K(k^2)\right\},$$

$$\Omega = \frac{\pi}{2K(k^2)} \quad \text{and} \quad k^2 = \frac{H+1}{2} \quad .$$

Further $$\phi = \frac{\pi}{4} \int_0^{\psi} \frac{d\psi}{\sqrt{k^2 - \sin^2 \psi/2}} \Big/ K(k^2)$$

and $$\psi = 4Kk/\pi \int cn\left(\frac{2K\phi}{\pi}\right) d\phi$$

$$= 4 \sum_{n=1}^{\infty} \frac{1}{(2n-1)} \sin (2n-1) \phi \Big/ \cosh\left\{(n-\tfrac{1}{2})\pi \frac{K'(k^2)}{K(k^2)}\right\} \quad . \tag{11}$$

Here E and K are the usual complete elliptic integrals, cn is the Jacobian elliptic function, and $K' = K\left(\sqrt{1-k^2}\right)$. Electrons trapped at the bottom of the well are represented by $k^2 = 0$. Barely trapped electrons have $k = 1$.

Since we are interested in the case of near resonance, we substitute Equation (11) into Equation (10), keeping only the resonant term $\phi - \alpha z'$. Introducing $\phi' = \phi - \alpha z'$ by a canonical transformation, we obtain the new autonomous Hamiltonian

$$H = 2k^2 - \alpha \frac{8}{\pi} \left| E - (1-k^2)K \right| - \frac{2\cos\phi'}{\cosh\left(\pi K'/2K\right)} \tag{12}$$

which is now a constant of motion.

The bottom of the potential well corresponds to $H' = 0$. If $|\cos\phi| < 1$ for all k^2 between zero and 1, then the orbit passing through the bottom of the well is connected to the top and most particles will be detrapped. Equation (10) is easily solved for $\cos\phi'$ and we find graphically that such detrapping is most likely to occur at $\alpha = 0.865$. In this case, $\beta < 0.1$ is found to lead to detrapping. Recall that we have previously noted that for $\alpha \approx 1$, $\beta = < \frac{1}{4} x_\beta^2 / x_o^2$. Thus total detrapping could be avoided for $x_\beta^2 / x_o^2 < 0.4$. But even in this case substantial detrapping could occur from electrons trapped away from the bottom of the well.

A more important limitation on predicted detrapping results from the finite length of the wiggler. We crudely estimate the detrapping of electrons from near the top of the well where $\pi K'/2K < 1$. From Equation (12),

$$\frac{dJ}{dz} = \frac{dz'}{dz}\frac{\partial H}{\partial \phi'} = 2\Omega_s \beta \frac{\sin \phi'}{\cosh (\pi K'/2K)} \leq 2\Omega_s \beta . \quad (13)$$

For a Gaussian beam using Equations (2) and (13) and putting $\alpha \approx 1$, we have

$$\frac{dJ}{dz} \lesssim 2k_\beta \frac{x_\beta^2}{x_o^2} \frac{Z/Z_R}{1 + (Z/Z_R)^2} . \quad (14)$$

Those electrons with J nearly equal to $J_{max} = 8/\pi$ may now be lifted over the top if J increases sufficiently.

Consider a wiggler of length 2L with optical waist at the center. Then we may obtain an estimate of the fraction of trapped phase space, $\Delta J/J_{max}$, which moves over the top of the well by integrating Equation (14) from $Z = 0$ to L. We take only the half length to account crudely for the fact that only half the electrons have phases leading to $dJ/dZ > 0$. Then the possible fractional detrapping is given by:

$$f = \frac{\Delta J}{J_{max}} \lesssim \frac{\pi}{8} \frac{x_\beta^2}{x_o^2} k_\beta Z_R \ln \left[\left(1 + (L/Z_R)^2\right)\right] . \quad (15)$$

Thus it would appear that only long wigglers with large $k_\beta Z_R$ can be subject to serious detrapping. This could put an important emittance constraint on long wigglers. However, we note that another such constraint is already conventionally taken into account in wiggler design. This arises from the fact that betatron motion at fixed γ leads to a change in electron longitudinal velocity and hence does not permit electrons to be trapped in the ponderomotive well. From Equation (8) we may write

$$\left(\frac{d\psi}{dz'}\right)_{eff} = \frac{k_s}{\Omega_s}\left(\frac{k_w a_w}{2\gamma} x_\beta\right)^2 < \sqrt{2}$$

the limit coming from the depth of the potential well in Equation (9). This means that the maximum allowable emittance, ε_{max} is determined from:

$$k_\beta Z_R \frac{x_{\beta max}^2}{x_o^2} = 2\sqrt{2} \quad . \tag{16}$$

Defining the maximum allowable emittance from Equation (16) and substituting into Equation ((13), we have for the fraction of detrapped phase space:

$$f \leq \frac{\pi}{4}\sqrt{2}\ln\left[1+\left(\frac{L}{Z_R}\right)^2\right]\frac{\varepsilon}{\varepsilon_{max}} \quad . \tag{17}$$

For the usual wiggler $L = Z_R$ and allowing approximately for the overestimates we have made, we conclude $f \sim 0.4\ \mathcal{E}/\mathcal{E}_{max}$ with a numerical factor uncertain by perhaps a factor of 2. Pending detailed simulations for specific designs, it seems clear that for $\mathcal{E}/\mathcal{E}_{max} < \frac{1}{2}$ the detrapping is not significant.

IV. SUMMARY AND CONCLUSIONS

We have studied the effect of 2-dimensional motion on electron "synchrotron" oscillations in the ponderomotive potential of a free electron laser. We find that the transverse motion of the electrons is essentially an unconstrained betatron oscillation. However, if the optical wave front is curved, this motion couples into the synchrotron oscillations. We find this coupling to be weak except near resonance where $2k_\beta = \Omega_s$ which occurs typically at peak circulating optical power levels near 1 GW. Under resonant conditions, the coupling is marginally strong enough to lead to some detrapping. Thus a detailed numerical simulation of specific cases may be required.

However, it appears that in an amplifier the parameters may change rapidly enough that the resonance is passed through without significant detrapping.[3] During the buildup phase of an oscillator passing through resonant power levels, we have roughly estimated peak potential detrapping to be of order of 40% if the emittance is the maximum allowed by other considerations. Hence, if a reasonable gain margin exists, this detrapping is not essential. With smaller emittances, the effect is of course smaller. For actual cylindrical cases where many orbits do not pass close to the axis, the effect is further reduced.

It should be noted that we have not studied the self-consistent effect of betatron motion on emission, but only the effect of an assumed wave shape on electron trapping. With these caveats we conclude that 2-dimensional effects do not seriously perturb the simple 1-dimensional picture of a free electron laser or introduce significant further design constraints.

It is a pleasure to acknowledge discussions with N. Kroll, R. Novick, D. Quimby, V. Wong and, particularly, D. Prosnitz.

REFERENCES

1. W. Colson, Phys. Quan. Elec., 8, 457 (1982).

2. N. Kroll, P. Morton, M. Rosenbluth, J. Quan. Elec., QE-17, 1436 (1981).

3. D. Prosnitz, private communication.